

# uS3/Rps3 controls fidelity of translation termination and programmed stop codon readthrough in co-operation with eIF3

Kristýna Poncová<sup>1,2</sup>, Susan Wagner<sup>1</sup>, Myrte Esmeralda Jansen<sup>1</sup>, Petra Beznosková<sup>1</sup>, Stanislava Gunišová<sup>1</sup>, Anna Herrmannová<sup>1</sup>, Jakub Zeman<sup>1</sup>, Jinsheng Dong<sup>3</sup> and Leoš Shivaya Valášek<sup>1,\*</sup>

<sup>1</sup>Laboratory of Regulation of Gene Expression, Institute of Microbiology of the Czech Academy of Sciences, Videnska 1083, 142 20 Prague, the Czech Republic, <sup>2</sup>Charles University, Faculty of Science, Prague, the Czech Republic and <sup>3</sup>Laboratory of Gene Regulation and Development, Eunice Kennedy Shriver National Institute of Child Health and Human Development, National Institutes of Health, Bethesda, MD 20892, USA

Received July 21, 2019; Revised October 03, 2019; Editorial Decision October 04, 2019; Accepted October 07, 2019

## ABSTRACT

Ribosome was long considered as a critical yet passive player in protein synthesis. Only recently the role of its basic components, ribosomal RNAs and proteins, in translational control has begun to emerge. Here we examined function of the small ribosomal protein uS3/Rps3, earlier shown to interact with eukaryotic translation initiation factor eIF3, in termination. We identified two residues in consecutive helices occurring in the mRNA entry pore, whose mutations to the opposite charge either reduced (K108E) or increased (R116D) stop codon readthrough. Whereas the latter increased overall levels of eIF3-containing terminating ribosomes in heavy polysomes *in vivo* indicating slower termination rates, the former specifically reduced eIF3 amounts in termination complexes. Combining these two mutations with the readthrough-reducing mutations at the extreme C-terminus of the a/Tif32 subunit of eIF3 either suppressed (R116D) or exacerbated (K108E) the readthrough phenotypes, and partially corrected or exacerbated the defects in the composition of termination complexes. In addition, we found that K108 affects efficiency of termination in the termination context-specific manner by promoting incorporation of readthrough-inducing tRNAs. Together with the multiple binding sites that we identified between these two proteins, we suggest that Rps3 and eIF3 closely co-operate to control translation termination and stop codon readthrough.

## INTRODUCTION

To ensure proper transfer of genetic information from genes into proteins, the ribosome has to accurately recognize not only the proper start (initiating codon) of the gene to be translated but also its end (one of the three stop codons). In this critical endeavor the ribosome is assisted by numerous proteins and protein complexes called eukaryotic initiation and release factors (for review see (1–3)). Naturally, the ribosomal components such as its rRNAs and ribosomal proteins participate in all four phases of the translational cycle (initiation – elongation – termination – recycling) (4,5), whereas the aforementioned factors have, with a few exceptions, only a single-phase-specialized roles. One such an exception is the initiation factor eIF3 (reviewed in (6)). Not only it coordinates the progress of most of the initiation steps (see e.g. (7–25)), it also fine tunes the fidelity of translation termination and promotes programmed stop codon readthrough (26,27) (see below).

During canonical termination the stop codon is decoded by the release factor 1 (eRF1) that enters the A-site of the 80S ribosome in complex with the GTP-binding protein eRF3 (reviewed in (3)). In eukaryotes, eRF1 recognizes all three stop codons (UAA, UAG and UGA). According to the most recent model, eRF3 senses the proper accommodation of eRF1 at the A-site occupied by the stop codon (28,29). This triggers GTP hydrolysis on eRF3, which then leaves the pre-termination complex to make room for the recycling factor called ABCE1 (RLI1 in budding yeast). Binding of ABCE1, a member of the ATP-binding cassette (ABC) family of proteins, promotes polypeptide release by pushing the GGQ motif of eRF1 into the peptidyl transferase center to stimulate the hydrolysis of ester bond between the nascent polypeptide chain and the CCA end of the peptidyl-tRNA sitting at the P site. This NTP-

\*To whom correspondence should be addressed. Tel: +420 241 062 288; Fax: +420 241 062 665; Email: valasekl@biomed.cas.cz

independent step captures the production of a particular protein.

However, in some specific cases, not all stop codons signal the proper end of translation, which can thus continue beyond to the next stop codon. Generally speaking, translation termination can be viewed as a constant competition between stop codon recognition by release factors and stop codon decoding by near-cognate tRNAs that infrequently results in stop codon readthrough and production of C-terminally extended protein isoforms, often with important biological roles (30–32). This competition differs genome-wide in its efficiency which can be influenced by many factors. For example, we recently demonstrated that each and every stop codon, together with its immediately following +4 nucleotide, defines a stop codon tetranucleotide that determines the specific decoding rules for so-called readthrough-inducing (rti)-tRNAs, the competition odds of which are preferentially increased at the defined tetranucleotides (33–35).

Beyond determining the rti-tRNA preference, the +4 nucleotide also appears to directly influence the eRF1-mediated stop codon decoding (32,36,37). In particular, the presence of a cytosine at the +4 position modestly, but significantly, interferes with eRF1 decoding of all three stop codons (33). Strikingly, we identified a similar role also for eIF3 (6,26,27). In particular, eIF3 appears to interfere with eRF1 recognition of stop codons at the third (wobble) position and, at the same time, it stimulates incorporation of rti-tRNAs with mismatches at this very position. In other words, by affecting the proper eRF1•eRF3•GTP accommodation, eIF3 enables greater competition of tetranucleotide-specific rti-tRNAs with wobble mismatches to boost efficiency of readthrough.

Expectedly, several ribosomal proteins have also been implicated in controlling fidelity of translation termination/readthrough, such as for example uS19/Rps15 and eS25/Rps25 (38,39); however, according to our knowledge, the molecular mechanism of their involvement is unclear. In this respect, uS3/Rps3 also deserves a particular attention, mainly from the following reasons:

- 1) It is situated in the head region of the solvent exposed side of the small ribosomal subunit at the mRNA entry channel reaching out to the decoding pocket (Figure 1A). Accordingly, some Rps3 mutations were shown to suppress frameshift and nonsense mutations in several tested genes by altering translational accuracy of ribosomes (40), whereas some others increased frameshifting at inhibitory CGA-CGA codon pairs (41). Based on the analogy to its bacterial counterpart, Rps3 was also proposed to be implicated in the helicase activity of the ribosome (42,43).
- 2) Being a part of the decoding pocket, Rps3 directly contacts the mRNA 3' of the A-site with its C-terminal tail (44–46). Several C-terminal Rps3 residues also appear to interact with 18S rRNA residues that form the 'mRNA entry channel latch' (a noncovalent interaction between rRNA nucleotides in helices 18 and 34 (47)), which plays a critical role during scanning for AUG selection. Binding of several eIFs to the free 40S subunit dissolves this latch (by releasing the contact between h18 in the 40S

body and h34 and uS3/Rps3 in the 40S head) to open the channel for mRNA loading and subsequent ribosomal scanning. The reversal latch closure on AUG recognition, which is triggered by the delicate interplay of these eIFs, then clamps on the mRNA and arrests scanning to enable a subsequent subunit joining step (reviewed in (2)).

- 3) During stop codon decoding, eRF1, sitting in the ribosomal A-site, was proposed to contact uS3/Rps3 via a part of its N-domain (48). Interestingly, Taylor *et al.* further proposed that one of the conformational changes induced by eRF1–eRF3–GMPPNP binding to the 80S pre-termination complexes (pre-TCs) involves a movement of h16 of 18S rRNA and the N-terminal domain (NTD) of Rps3 toward each other, which results in the establishment of a new head–body connection on the 40S solvent side and a constriction of the mRNA entrance. Noticeably, this constriction, occurring in the terminating 80S couples, mechanistically resembles an aforementioned rearrangement of the similar latch components of the 48S pre-initiation complex (PIC) upon AUG selection during initiation.
- 4) uS3/Rps3 interacts with the NTD of g/Tif35 and the C-terminal domain (CTD) of a/Tif32 subunits of yeast eIF3 (8,12). Mutations in the a/Tif32-CTD (which interacts also with h16–18 of 18S rRNA (49)) and g/Tif35 confer phenotypes indicating destabilization of the open/scanning conducive latch state, as well as phenotypes suggesting the opposite effect of destabilizing the closed/scanning arrested latch conformation (8,12). Similarly, mutations of Rps3 residues that interact with mRNA and rRNA residues of the entry channel were also shown to decrease stability of the closed latch state and diminish recognition of near-cognate initiation sites *in vivo* (50). In addition, they were also implicated in stabilizing mRNA interactions with the PICs at the entry channel in a functionally redundant way with eIF3-dependent stabilization of the PIC–mRNA interactions at the exit channel (50). Consistently, stable binding of mRNAs with very short UTRs containing the TISU element to 43S PICs was also shown to rely primarily on the interaction of their +6 nt with Rps3 (51). Altogether, these findings indicate a close co-operation between eIF3 and Rps3 in stabilizing the mRNA at the both channels of the mRNA binding path, as well as in the close-to-open/open-to-close latch acrobatics during the initiation phase (6).

Taken altogether plus the fact that the aforementioned mutations in the a/Tif32 and g/Tif35 subunits of eIF3 also affect fidelity of termination (26,27), it is tempting to speculate that the constriction of the mRNA entrance tunnel during termination involves similar actors and serves the similar purpose; i.e. to clamp the mRNA into the mRNA entry pore to stabilize the termination complex as it prepares for the peptide release, which has never been examined.

Here, we subjected Rps3 to site directed mutagenesis and isolated two mutants with the opposite readthrough phenotypes that genetically interacted with the readthrough-reducing mutations at the extreme C-terminus of the a/Tif32 subunit of eIF3 and impacted on the composition

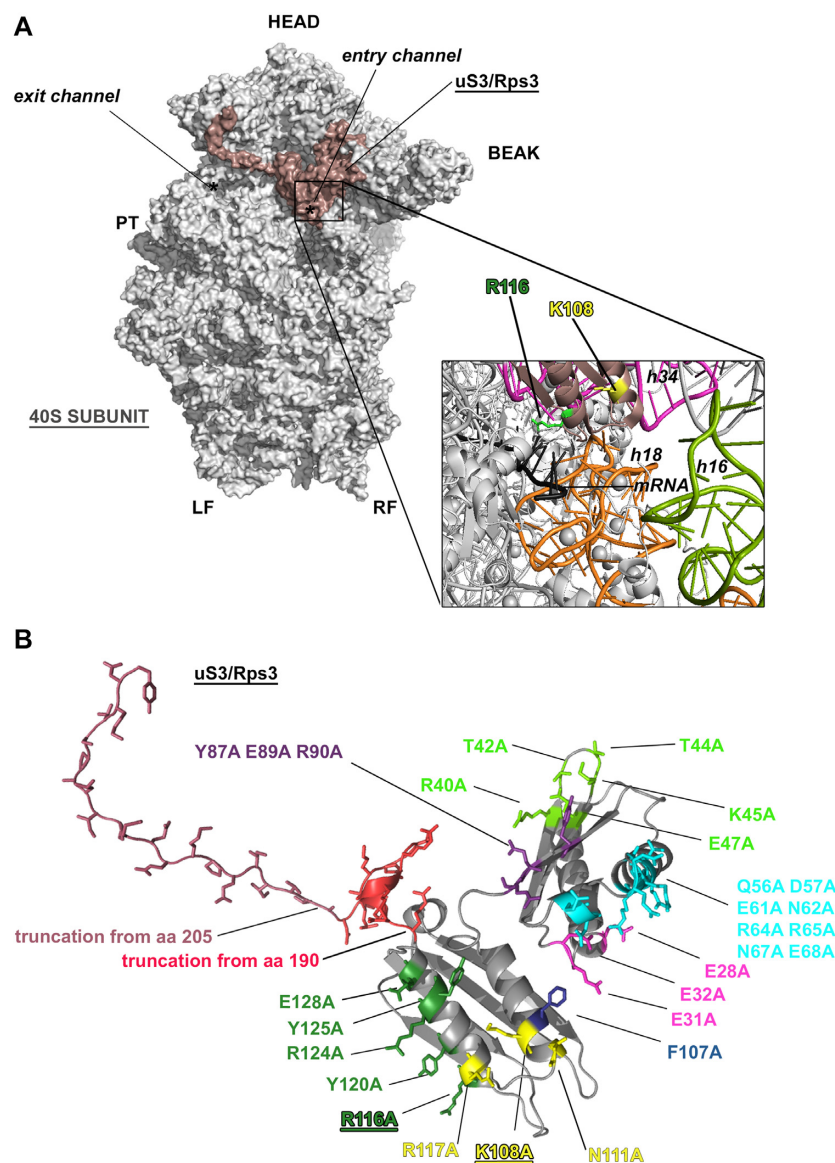


**Figure 1.** Rps3 of the small ribosomal subunits and the schematic of its site-directed mutagenesis. (A) The position of Rps3 in the context of the small ribosomal subunit shown from its solvent-exposed side (PDB ID 3J81); Rps3 is shown in bronze with positions of R116 and K108 highlighted in the magnified frame; mRNA is shown in black and helices 16, 18 and 34 of 18S rRNA in green, orange and violet, respectively. (B) All Rps3 residues that were mutated/deleted either individually or in blocks in this study are displayed in the Rps3 secondary structure (PDB ID 4V88).

of the pre-termination complexes. Detailed analysis of one of these mutations suggested that the K108 residue of Rps3 affects efficiency of termination in the +4 base-specific manner by promoting incorporation of rti-tRNAs at the ribosomal A-site. Finally, we also identified three direct contacts between uS3/Rps3 and a/Tif32 and propose a molecular mechanism of their co-operative involvement in the control of termination fidelity.

## MATERIALS AND METHODS

### Yeast strains and plasmids

The lists and descriptions of yeast strains, plasmids, and primers used throughout this study (summarized in Supple-

mentary Tables S2–S4) can be found in the Supplementary data.

### Stop codon readthrough assays

Majority of stop codon readthrough assays in this study were performed using a standard bicistronic reporter construct bearing a *Renilla* luciferase gene followed by an in-frame firefly luciferase gene, originally developed by (52). Separating the two genes is either a tetranucleotide termination signal (UGA-C) or, for control purposes, the CAA sense codon followed by cytosine. In indicated cases, the termination signal and/or the following nucleotide context was modified. It is noteworthy that this system avoids possible artifacts connected to the changes in the efficiency of

translation initiation associated with the nonsense mediated decay (NMD) pathway (53), because both *Renilla* and firefly enzymes initiate translation from the same AUG codon. For further details please see (54,55). All experiments and data analyses were carried out according to the Microtiter plate-based dual luciferase protocol developed by (56) and commercially distributed by Promega. Readthrough values are represented as mean  $\pm$  SD from triplicates ( $n = 6$ ) and each experiment was repeated at least three times. The raw data for all dual luciferase assays (absolute luciferase activities) are given in the Supplementary Excel File.

### Polysomal gradient analysis

For polysome profile analysis, strains were grown in yeast extract-peptone-dextrose (YPD) at 30°C to O.D.<sub>600</sub> of  $\sim 1$ . Cycloheximide (50  $\mu\text{g/ml}$ ) was added 5 min prior to harvesting, and WCEs were prepared in the breaking buffer composed of 20 mM Tris-HCl, pH 7.5, 50 mM KCl, 10 mM MgCl<sub>2</sub>, 1 mM dithiothreitol [DTT], 1 mM phenylmethylsulfonyl fluoride [PMSF] and 1 $\times$  Complete Protease Inhibitor Mix tablets without EDTA [Roche]. Cells were broken by FastPrep Instrument (MP Biomedicals) at the intensity level of 5 in two 20 s cycles. Fifteen A<sub>260</sub> units of WCEs were separated by high velocity sedimentation on a 5–45% sucrose gradient by centrifugation at 39 000 rpm for 2.5 h in a SW41Ti rotor (Beckman Coulter). The resulting gradients were scanned at A<sub>254</sub> to visualize ribosomal species using Teledyne ISCO UA-6 UV/VIS gradient detector.

### Heavy polysomal gradient analysis

For analysis of complexes associated with pre-termination ribosomes, strains were grown in (YPD) at 30°C to O.D.<sub>600</sub> of  $\sim 1$ . Cycloheximide (50  $\mu\text{g/ml}$ ) was added 5 min prior to harvesting, the cells were subsequently cross-linked with 0.5% formaldehyde (HCHO) for 30 min on ice and WCEs were prepared as described in the previous chapter. Hundred A<sub>260</sub> units of the resulting WCEs were loaded on 5–45% sucrose gradient and separated by centrifugation at 16 800 rpm for 13.5 h in a SW 32-Ti Beckmann rotor. The heaviest polysomal fractions (pentasomes and more) were collected, pooled and treated with RNase I to separate the pre-initiation complexes (PICs) from 80S couples on actively translated mRNAs. Thus treated samples were subjected to the second round of sucrose gradient (5–45%) centrifugation according to the resedimentation protocol described before (27). The resolved 80S couples—enriched in termination complexes—were collected, loaded in five two-fold dilutions onto the SDS-PAGE gel and processed for western blot analysis with the indicated antibodies. Western blot signals from each of the five two-fold dilutions obtained with individual antibodies were quantified by Quantity One and plotted against their corresponding loadings. Individual slopes (representing relative amount of each factor in mutant cells) calculated from the linear regression of resulting plots were normalized to the slope obtained with the *TIF32 RPS3* wt strain, which was set to 100%.

### GST pull-down experiments

GST pull-down experiments with GST fusions and *in vitro*-synthesized [<sup>35</sup>S]-labeled polypeptides (see Supplementary Table S2 for vector descriptions) were conducted as follows. Individual GST-fusion proteins were expressed in *Escherichia coli*, immobilized on glutathione-Sepharose beads and incubated with 10  $\mu\text{l}$  of <sup>35</sup>S-labeled potential binding partners at 4°C for 2 h. The beads were washed 3 times with 1 ml of phosphate-buffered saline, and bound proteins were separated by SDS-PAGE. Gels were first stained with Gel-code Blue Stain Reagent (Pierce) and then subjected to autoradiography.

## RESULTS

### Rps3 mutations in two helices running in parallel cause opposite stop codon readthrough phenotypes

To examine the role of Rps3 in translation termination, we selected majority of surface-exposed segments of Rps3 and individually replaced each of these segments with a string of the corresponding number of alanine residues (to shorten the side chain) in the fully functional *RPS3* allele bearing the FLAG tag at its N-terminus (to facilitate its detection by Western blotting). All mutations, summarized in the color-coded arrangement in Figure 1B, were generated in the *RPS3* allele under the control of the standardized *RPS28* promoter (57) on a single copy plasmid and introduced into a yeast strain deleted for the chromosomal copies of *RPS3* and *TIF32* (the latter encoding the  $\alpha$ /Tif32 subunit of yeast eIF3) bearing the wt alleles on separate covering plasmids by plasmid shuffling. After the eviction of the *RPS3* covering plasmid, all mutants except for the C-terminal truncations *rps3-I-190* (lethal, same as the *rps3-I-200* allele shown before (58)) and *rps3-I-205* (severe Slow-growth [Slg<sup>-</sup>] phenotype) were scored for the stop codon readthrough phenotype as described before (27). (Surprisingly, none of the Ala-substituting mutations displayed any significant growth phenotype – see Supplementary Table S1).

Briefly, a standard way to measure the efficiency of stop codon readthrough is by the dual-luciferase reporter assay specifically designed to be independent of mRNA level changes (54). In this reporter system, two genes encoding luciferases are separated by an in frame stop codon or by the CAA coding triplet as a reference (Figure 2A). To increase the sensitivity of this assay, the UGA stop codon with the C at the 4<sup>th</sup> position in the UGA-CCG-UUC hexanucleotide, which is known to allow relatively high levels of readthrough, is typically used (59). In addition, we used the UGA-hexanucleotides from genes known to undergo programmed stop codon readthrough, like the UGA-CAA-UUA TMV-6nt context from the tobacco mosaic virus (TMV, whose genuine sequence is UAG-CAA-UUA) (60), which had the highest levels of readthrough from our selection. Among cellular genes from the *Saccharomyces cerevisiae* genome, we picked the programmed UGA-CAA-GAA hexanucleotide of *PDE2* (61), as well as the UGA-AUA-AAU hexanucleotide taken from the *SUP45* gene known for its highly efficient termination (27).

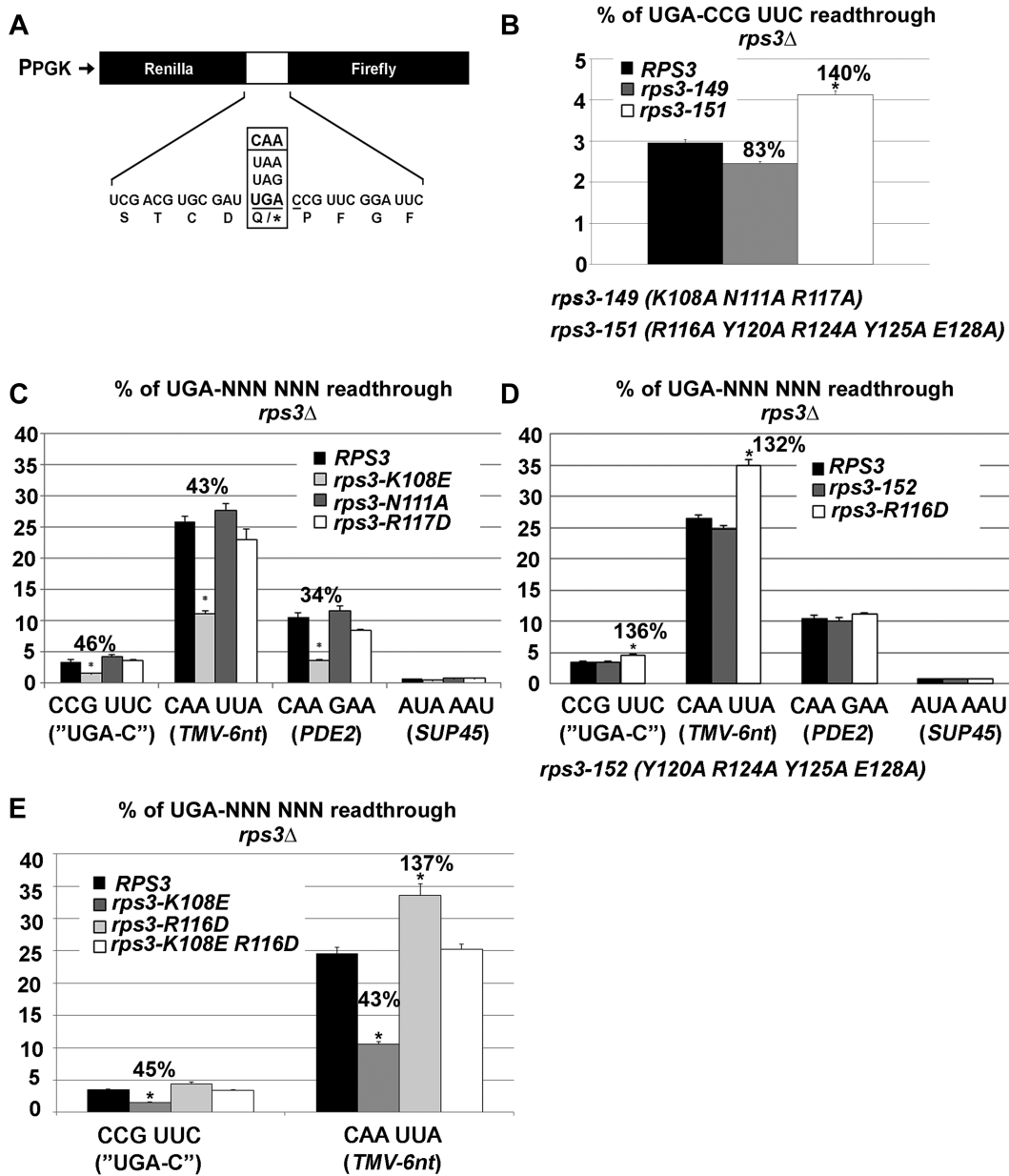


**Figure 2.** Rps3 mutations in two helices running in parallel cause opposite stop codon readthrough phenotypes. (A) Schematics of the standard dual luciferase readthrough reporter constructs with variable stop codons (or a CAA coding codon) under the PPGK promoter adapted from (27). (B–E) The *rps3* $\Delta$  strains ME166 bearing the indicated *rps3* mutant alleles on a single copy plasmid were introduced with the indicated dual luciferase readthrough reporter constructs (pTH477 as 'UGA-C'; PBB82 for TMV-6nt context; PBB84 for PDE2; and PBB85 for SUP45), grown in SD and processed for stop codon readthrough measurements as described in Materials and Methods. Statistical significance determined by the Student's *t*-test is indicated ( $P < 0.05$ ).

From all segment mutations that we tested (Supplementary Table S1), only the *rps3-149* K108A N111A R117A and *rps3-151* R116A Y120A R124A Y125A E128A displayed significant effects. The former reproducibly decreased readthrough by  $\sim 20\%$ , whereas the latter increased it by  $\sim 40\%$  (Figure 2B). To determine what residue(s) are responsible for these phenotypes, we individually substituted each of these 8 residues either with alanine or with a residue of an opposite charge, subjected them to the readthrough assay and found that *rps3-K108E* significantly (by  $\sim 50\text{--}70\%$ ) decreased readthrough at all three tested hexanucleotides (Figure 2C), whereas *rps3-R116D* increased it,

especially with the TMV-6nt context (by  $\sim 35\%$ ) (Figure 2D). Interestingly, the *rps3-R116A* substitution showed no readthrough when tested alone (data not shown), suggesting the importance of the given charge.

Please note that in agreement with an earlier study (50), the expression levels of the mutant proteins, as well as their incorporation into 40S subunits, were unchanged compared to the wild-type (wt) cells (Supplementary Figure S1A and B), they produced no obvious growth phenotypes (Supplementary Figure S1C), did not significantly affect expression from the control reporter plasmid (Supplementary Figure S1D), only conferred moderate reductions in

the ratio of polysomes to 80S monosomes that we measured in cycloheximide-stabilized extracts resolved by sedimentation through sucrose gradients (Supplementary Figure S1E). Also, no perturbation to the ratio of free 40S to free 60S subunits was evident except for a modest reduction in the *R116D* mutant. Taking into account that Rps3 is an essential protein whose absence from or altered placement in the 40S body would cause either cell death or severe growth defects, together these data clearly demonstrate that the observed readthrough phenotypes are caused by its impaired functioning as part of the small ribosomal subunit and not from its altered protein levels or defects in 40S biogenesis and/or stability.

Interestingly, K108 and R116 are situated next to each other on the opposite alpha helices ( $\alpha 4$  and  $\alpha 5$ , respectively) running in parallel, with their side chains facing into different planes (Figure 1A). R116 was proposed to directly contact mRNA (50), whereas K108 seems to lie in the vicinity of helix 34 (Figure 1A). Strikingly, combining these two mutations with the opposite readthrough phenotypes in a single *rps3-K108E R116D* allele resulted in a complete suppression of their individual phenotypes (Figure 2E). This may suggest that they play antagonistic roles during translation termination, perhaps thanks to their differing contacts in the mRNA entry pore.

### Mutating the extreme C-terminus of a/Tif32 reduces the readthrough efficiency

We previously showed that the C-terminal domain of a/Tif32 (residues 791–964), represented by an extended alpha-helix forming the flexible arm under the 40S beak (Figure 3A), interacted with uS5/Rps2 and uS3/Rps3 *in vitro* (12). To examine whether the a/Tif32-CTD—thanks to this interaction—also impacts on fidelity of termination like the a/Tif32-NTD does (26,27), we introduced Ala substitutions in consecutive blocks of 10 residues between amino acids 792 and 964 (dubbed boxes 16–33). To meet this ‘10 residues at a time’ rule and cover the entire region, the last two boxes (32 and 33) overlap by six residues (Figure 3B). All mutations were generated in the low copy pRS-plasmid-borne *TIF32-His*, encoding His<sub>8</sub>-tagged a/Tif32, and introduced into the *rps3Δ tif32Δ* strain by plasmid shuffling. None of these mutations was lethal, allowing eviction of the resident *TIF32<sup>+</sup> URA3* plasmid on medium containing 5-fluoroorotic acid (5-FOA). Surprisingly, only one of the resulting mutant transformants (box33) displayed some growth phenotype (moderate Slg<sup>-</sup>; Figure 3C and data not shown). Since it overlaps with box32, we subjected these two mutants to our readthrough assay and showed that they both reduced readthrough; *tif32-box33* conferred more pronounced reduction (by ~35%; Figure 3D). Neither of the observed phenotypes was caused by abnormalities in their expression levels (Figure 3E) or a significant impairment of translation efficiency (Supplementary Figure S1C). Taking into account that the C-terminus of Tif32 (namely residues 792–964 encompassing both boxes) does not make any contacts with other eIF3 subunits and, as such, is dispensable for the eIF3 integrity *in vivo* (24,62,63), our findings indicate that the contact between the a/Tif32-CTD and

uS3/Rps3 could indeed directly modulate the termination efficiency.

### Analysis of the genetic and physical interaction between the a/Tif32 C-terminal mutations and rps3-R116D

To investigate the prospective interplay between the a/Tif32-CTD and Rps3 in translation termination, we first combined both box mutations (reducing readthrough) with *rps3-R116D* (increasing readthrough) in the *rps3Δ tif32Δ* strain and subjected the resulting double mutants to the readthrough assay. In analogy to combining *rps3-K108E* (reducing readthrough) with *R116D* (increasing readthrough) (Figure 2E), combining *a/tif32-box33* with *rps3-R116D* resulted in a nearly complete suppression of their individual phenotypes (Figure 4A), suggesting antagonistic roles. A similar effect, although not statistically significant, was also observed with the *a/tif32-box32 rps3-R116D* double mutant. Interestingly, despite the termination efficiency correction, the *rps3-R116D* mutation exacerbated Slg<sup>-</sup> of *a/tif32-box33* indicating a more complex genetic interaction between these two proteins (Figure 4B).

Next, we examined the physical interaction between the a/Tif32-CTD and Rps3. As shown in Figure 5A and B, the [<sup>35</sup>S]-labelled *rps3-R116D* mutant dramatically reduced (by ~90%) binding to the wt a/Tif32-CTD (residues 791 through 964) fused to the GST moiety. Similarly, both box mutations diminished affinity towards wt Rps3 by robust ~80% (Figure 5A and C). However, since practically the identical reductions were also observed when both box mutations were combined with R116D (Figure 5A–C), it is clear that the a/Tif32-CTD–Rps3 interaction is mediated by at least two independent contacts; one mediated by R116 of Rps3 and the other by the extreme CTD of Tif32. In agreement, *rps3-R116D* fused to GST reduced binding to the full length a/TIF32 by ~35% compared to the wt Rps3 protein, regardless the presence of the box32 mutation ([<sup>35</sup>S]-labelled box33 mutant did not stably express *in vitro*) (Figure 5D and E). Interestingly, box32, when introduced into the full-length a/Tif32 protein, reduced binding to both wt Rps3 or R116D by ‘only’ ~50% (Figure 5D and F), compared to ~80% in case of a/tif32-CTD-box32, suggesting the presence of even a third contact upstream of the a/Tif32-CTD. Existence of the third contact would also explain the difference in binding affinity of *rps3-R116D* against the a/Tif32-CTD (~90% reduction; Figure 5A) versus the full length a/Tif32 protein (~35% reduction; Figure 5E). Indeed, we found that the a/Tif32-NTD segment encompassing residues 200–396 strongly and specifically interacted with Rps3 (Figure 5G), moreover, in the R116- and K108-independent manner (Figure 5H). These findings suggest a delicate network of contacts between these two binding partners that could stimulate and/or be a part of critical conformational changes that ribosome undergoes during termination (as well as initiation) in this important region, as described in the introduction.

### Analysis of the genetic and physical interaction between the a/Tif32 C-terminal mutations and rps3-K108E

Next we combined both *tif32-box* mutations (reducing readthrough) with *rps3-K108E* (also decreasing

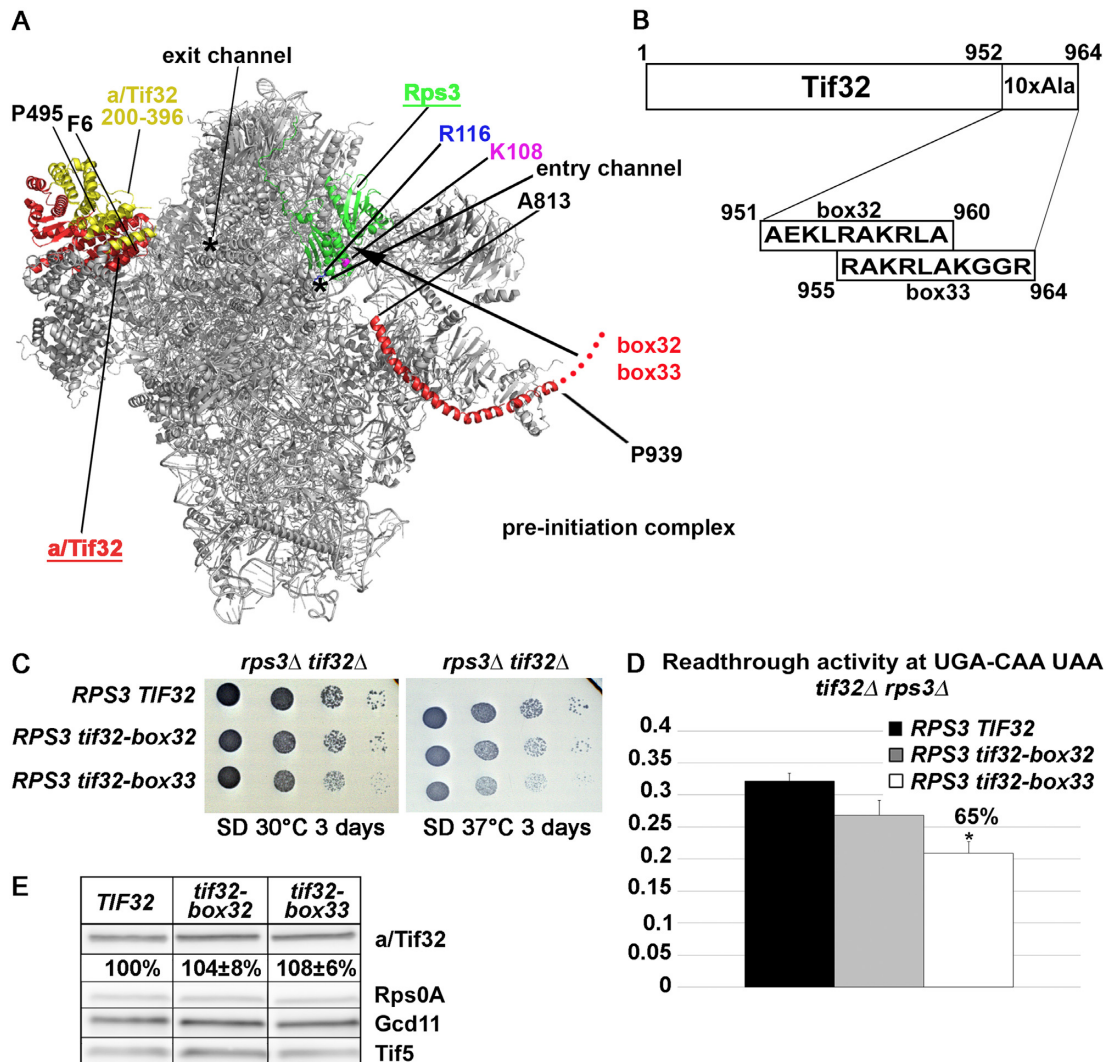


**Figure 3.** Mutating the extreme C-terminus of a/Tif32 reduces the readthrough efficiency. (A) Positions of Rps3 and the structure-solved/modelled parts of the a/Tif32-NTD and -CTD (defined by the amino acid coordinates) in the context of the small ribosomal subunit shown from its solvent-exposed side (PDB ID 6FYU); Rps3 is shown in green with positions of R116 and K108 highlighted; a/Tif32 in red with the residues 200–396 highlighted in yellow and the putative placement of the extreme C-terminal boxes 32 and 33 indicated. The interaction between the latter boxes and Rps3 identified in this study is illustrated by an arrow. (B) The schematic of the a/Tif32 protein depicting the amino acid residues that were substituted with a stretch of alanines in the a/tif32-box32 and -box33 mutants. (C) The a/tif32-box33 mutation causes a mild slow growth phenotype. Transformants of KPH31 (*rps3Δ tif32Δ*) bearing the indicated wt or mutant *TIF32* alleles were spotted in four serial 10-fold dilutions on SD medium and incubated at 30°C and 37°C. (D) Mutating the extreme C-terminus of a/Tif32 reduces the readthrough efficiency. Transformants of KPH31 (*rps3Δ tif32Δ*) bearing the indicated wt or mutant *TIF32* alleles were introduced with the control (pTH477) dual luciferase readthrough reporter construct processed for stop codon readthrough measurements as described in Figure 2B. Statistical significance determined by the student's *t*-test is indicated ( $P < 0.05$ ). (E) Neither of the box mutations of a/Tif32 alters its steady state protein levels. Transformants of KPH31 (*rps3Δ tif32Δ*) bearing the indicated wt or mutant *TIF32* alleles were grown in the YPD medium at 30°C to an  $OD_{600} \sim 1$ , and WCEs were prepared and subjected to western blot analysis with antibodies indicated on the right side of the panel. Western blot signals were quantified by Quantity One and the relative Tif32 protein levels from three biological replicates were normalized to the Rps0A loading control.

readthrough) in the *rps3Δ tif32Δ* strain and observed a statistically significant additive effect; i.e. exacerbation of the negative stop codon readthrough in the *tif32-box33 rps3-K108E* double mutant (Figure 6A), which did not manifest itself into a growth defect (Figure 6B). A similar effect was also observed with the *a/tif32-box32 rps3-K108E* double mutant. In contrast to R116D, the K108E mutation showed a smaller impact on the a/Tif32–Rps3 interaction (reduction by ~50%; Figure 7A–C), which was seen only with the a/Tif32-CTD construct but not with the full-

length protein (Figure 7D and E). These findings indicate that both RPS3 residues under investigation interact with a/Tif32 by different means (speaking for altogether four points of contact) and, at the same time, that the cooperation between K108 of Rps3 and the extreme C-terminus of a/Tif32 to fine tune the fidelity of termination has more functional than a physical character.

The R116D mutation was—thanks to its initiation phenotype—earlier shown to reduce expression levels of eIF1 (50). Even though eIF1 has never been implicated in

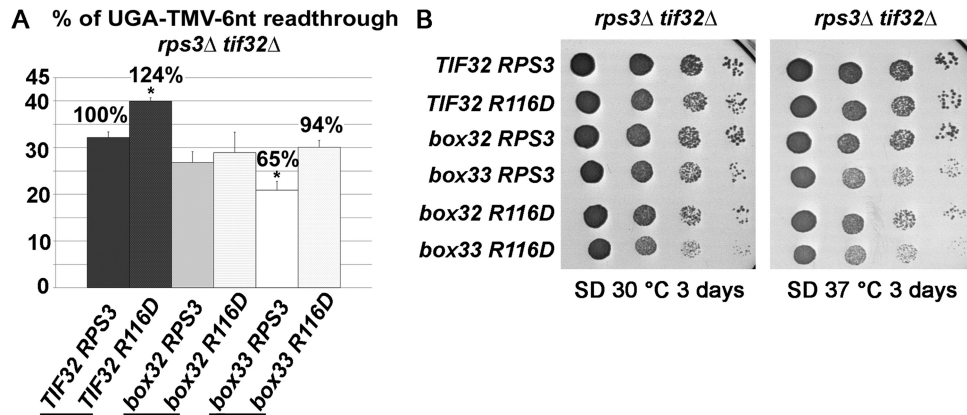


**Figure 4.** Analysis of the genetic interaction between the a/Tif32 C-terminal mutations and *rps3*-R116D. (A) Combining a/*tif32*-*box33* with *rps3*-R116D results in a complete suppression of their individual readthrough phenotypes. Transformants of KPH31 or KPH46 (*rps3* $\Delta$  *tif32* $\Delta$ ) bearing the indicated wt or mutant *TIF32* and *RPS3* alleles were introduced with the TMV-6nt context (PBB82) dual luciferase readthrough reporter construct processed for stop codon readthrough measurements as described in Figure 2B. Statistical significance determined by the student's *t*-test is indicated ( $P < 0.05$ ). (B) Combining a/*tif32*-*box33* with *rps3*-R116D further exacerbates the Slg<sup>-</sup> of the former mutant. Transformants of KPH31 (*rps3* $\Delta$  *tif32* $\Delta$ ) bearing the indicated wt or mutant *TIF32* and *RPS3* alleles were spotted in four serial 10-fold dilutions on SD medium and incubated at 30°C and 37°C.

termination, we overexpressed eIF1 in mutant strains bearing R116D or K108E to show that prospective changes in eIF1 levels do not impact efficiency of readthrough, which was indeed the case (Supplementary Figure S2).

#### The intact K108 residue of Rps3 is important for Cys-rti-tRNA incorporation at the UGA stop codon in the +4 base-specific manner

We recently demonstrated that the +4 base immediately following each of the three stop codons determines the so-called stop codon tetranucleotide decoding rules; i.e. how efficiently a tRNA that is near-cognate to a given stop codon will incorporate at the A-site occupied by it. Based on these rules we designated near-cognate tRNAs with high specificity for selected tetranucleotides as rti-tRNAs (33–35). However, the molecular mechanism of this preference is not known. In addition, we previously showed that eIF3 associates with pre-termination complexes where it interferes with the eRF1 decoding of the third or wobble position of the stop codon set in the unfavorable termination context and thus allows incorporation of rti-tRNAs with a mismatch at the same position (26,27). Since Rps3 interacts with eIF3 (12) and also contacts mRNA 3' of the A-site (44–46), we wished to examine whether Rps3 also stimulates incorporation of rti-tRNAs to the A-site in the tetranucleotide-specific manner, perhaps in co-operation with eIF3, and thus contributes to setting the stop codon tetranucleotide decoding rules.

To do that, we overexpressed all four rti-tRNAs (Cys, Trp, Gln and Tyr) in both *rps3* mutant strains and measured readthrough at all four UGA-N stop codon tetranucleotides, as well as at UAG-C and UAA-C (Figure 8). The overexpression strategy has been routinely used in our laboratory to magnify the effect of the rti-tRNA of interest (27,33–35). First, comparing the readthrough effects on the aforementioned tetranucleotides in cells expressing only the empty vector (EV), we noticed that R116—despite being in contact with mRNA's bases representing the termination

context 3' of the A-site—increases readthrough independently of the type of stop codon as well as of the +4 base identity when substituted with Asp (Figure 8A–G; 'EV' bars). In contrast, K108E showed the strongest preference for the programmed UGA-C (Figure 8A and G; 'EV' bars), less strong for UGA-G and the other two stops (UAG-C and UAA-C) (Figure 8B, E and F; 'EV' bars), and with the remaining two UGA-A and -U tetranucleotides it displayed either no effect or even a modest increase (Figure 8C and D; 'EV' bars). These data suggest that K108, in contrast to R116, affects efficiency of termination in the +4 base-specific manner, perhaps allosterically via its prospective interaction with helix 34 (Figure 1A).

In the past, we showed that rti-tRNA<sup>Trp</sup> is the specific readthrough substrate for the UGA-A tetranucleotide *in vivo* and rti-tRNA<sup>Cys</sup> is preferred at UGA-G, while at UGA-C and UGA-U both rti-tRNAs are incorporated (33). The rti-tRNA<sup>Tyr</sup> is capable of inducing readthrough at all four UAA-N tetranucleotides but only at the single UAG-C tetranucleotide, whereas tRNA<sup>Gln</sup> does not markedly affect readthrough at the UAA-N tetranucleotides, instead it robustly increases readthrough at all four UAG-N tetranucleotides (35). Comparing values between 'EV' and 'hc tC(GCA)P1' (Figure 8A–D), it can be seen that K108E interferes with the Cys-rti-tRNA incorporation at UGA-C, -G and -U (i.e. those tetranucleotides that are preferred by this tRNA with an 'EV *versus* hc tC(GCA)P1' difference of ~1.7-fold), but not so much at UGA-A, where this difference is only ~1.3-fold. Incorporation of Tyr-rti-tRNA at UAA-C was impaired only modestly (Figure 8F), whereas Gln-rti-tRNA at UAG-C and Trp-rti-tRNA at UGA-N showed no effect at all (Figure 8E, G, and data not shown). In contrast, R116D interferes with incorporation of neither of all four rti-tRNAs at the examined tetranucleotides (Figure 8). To further support the specificity of our findings we examined similar effects with the control *rps3*-N111A mutation and observed no difference (Supplementary Figure S3). Hence we propose that K108 affects efficiency of termination by promoting in-

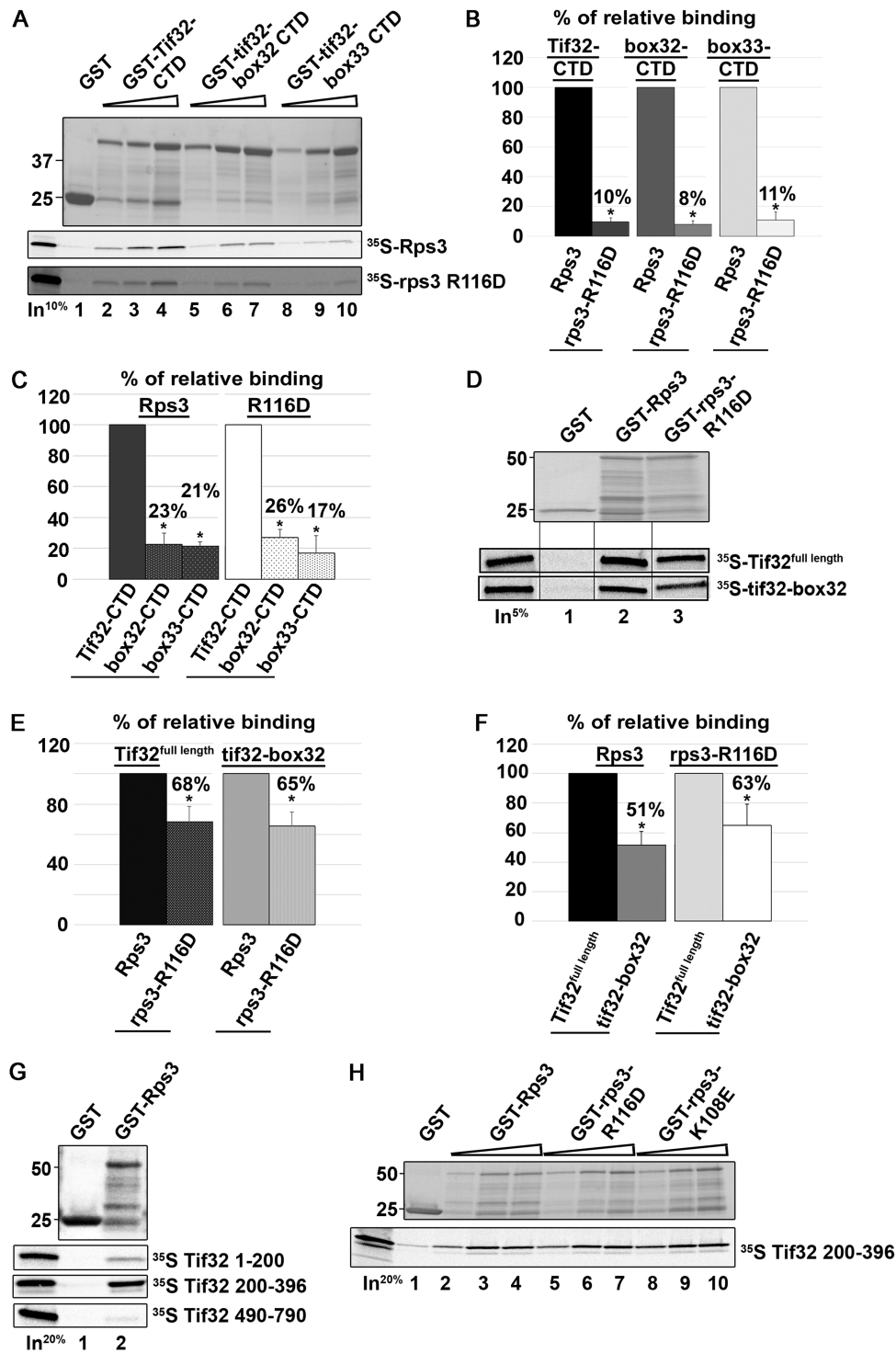


**Figure 5.** Analysis of the physical interaction between the  $\alpha$ /Tif32 C-terminal mutations and rps3-R116D. (A–F) Both *tif32-box* mutations, as well as *rps3-R116D* impair the  $\alpha$ /Tif32-Rps3 interaction independently of each other. The indicated wt or mutant proteins (or their segments) were fused to the GST moiety and together with the GST alone control tested for binding to the indicated [<sup>35</sup>S]-labeled proteins or their mutant derivatives. (In) indicates input amounts of proteins added to each reaction. The plots represent average values obtained from analysis of at least 3 GST-pull down experiments; standard deviations are given. Statistical significance determined by the student's *t*-test is indicated ( $P < 0.05$ ). (G–H) The  $\alpha$ /Tif32-NTD segment encompassing residues 200–396 interacts with Rps3 in the R116- and K108-independent manner. The indicated wt or mutant Rps3 protein was fused to the GST moiety and together with the GST alone control tested for binding to the indicated [<sup>35</sup>S]-labeled fragments of  $\alpha$ /Tif32. (In) indicates input amounts of proteins added to each reaction.

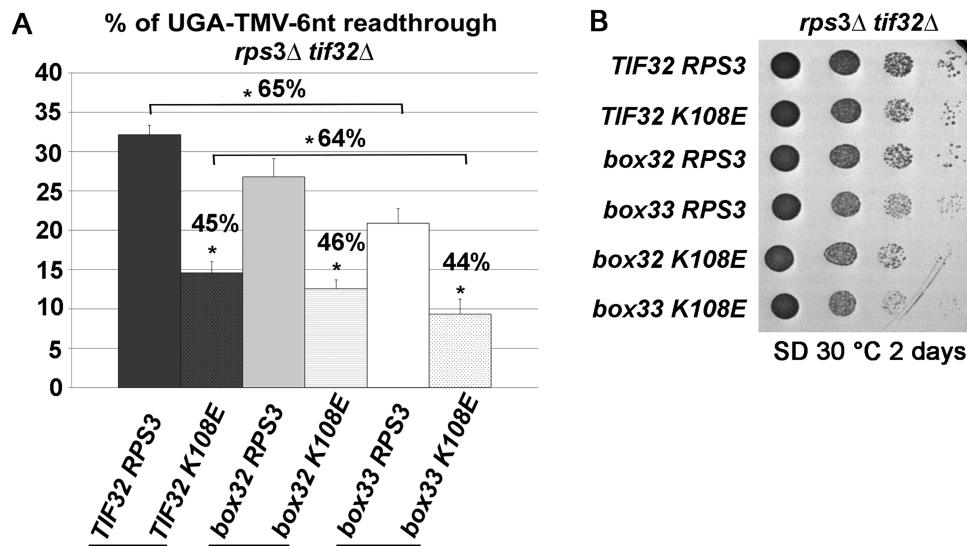


**Figure 6.** Analysis of the genetic interaction between the *a/Tif32* C-terminal mutations and *rps3*-K108E. (A) Combining *a/tif32*-*box* mutations with *rps3*-K108E exacerbates the negative stop codon readthrough phenotype of the individual mutants. Transformants of KPH31 or KPH46 (*rps3Δ tif32Δ*) bearing the indicated wt or mutant *TIF32* and *RPS3* alleles were introduced with the TMV-6nt context (PBB82) dual luciferase readthrough reporter construct processed for stop codon readthrough measurements as described in Figure 2B. Statistically significance determined by the Student's *t*-test is indicated ( $P < 0.05$ ). (B) Combining *a/tif32*-*box32* with *rps3*-K108E has no effect on the  $\text{Slg}^-$  of the former mutant. Transformants of KPH31 or KPH46 (*rps3Δ tif32Δ*) bearing the indicated wt or mutant *TIF32* and *RPS3* alleles were spotted in four serial 10-fold dilutions on SD medium and incubated at 30°C.

corporation of Cys-rti-tRNA (and to a smaller extent also of Tyr-rti-tRNA) in the stop codon tetranucleotide-specific manner, most likely in co-operation with eIF3.

#### The readthrough stimulatory effect of the K108 residue requires proper conformation of the decoding center

Binding of the aminoglycoside antibiotic paromomycin to pre-TCs causes displacement of the A1493 phosphate group relaxing the A-site codon decoding pocket. As a result, paromomycin changes the deformation of the near-cognate codon-anticodon helix, after which the ribosome does not actively sense the correct Watson-Crick base-pairing geometry and thus does not discriminate against near-cognate tRNAs (64). We previously showed that the effect of wt eIF3 on programmed stop codon readthrough, as described above, is nullified by the presence of paromomycin in pre-TCs, and proposed that eIF3 can no longer promote readthrough if the geometry of the decoding center is perturbed (27). Hence, to further support our favored idea that K108 directly co-operates with eIF3 during termination, we investigated the efficiency of UGA-C readthrough in *RPS3* wt versus mutant cells in the presence of 400  $\mu\text{g/ml}$  paromomycin. Consistent with previous results, we observed increased readthrough efficiency in the presence of paromomycin in all three strains (Figure 8H). Strikingly, whereas the magnitude of the readthrough modulation by R116D did not change at all under control *versus* paromomycin conditions (138% increase), paromomycin treatment nearly nullified the negative stop codon readthrough effect of K108E when compared to *RPS3* wt cells (Figure 8G). Since practically the same 'masking' effect was observed with eIF3 mutants before, we propose that whereas the mechanism by which R116 impacts on the fidelity of

termination does not depend on the intact A-site, the readthrough stimulatory effect of the K108 residue requires proper conformation of the decoding center, as in case of eIF3.

#### The *rps3*-K108E and -R116D mutations display opposite effects on the composition of pre-termination complexes *in vivo*

We showed previously that eIF3 associates with pre-termination 80S complexes (pre-TCs) in the manner dependent on the presence of termination factors eRF1 and eRF3 (26,27). To investigate how the *rps3* mutations, as well as the *a/tif32*-*box33* mutation affect the composition of pre-TCs, if at all, we analyzed the amounts of factors bound to the 80S couples isolated from heavy polysomes using the re-sedimentation protocol described previously (26,27,65). Briefly, whole cell extracts (WCEs) derived from formaldehyde cross-linked cells were resolved on sucrose gradients after high velocity centrifugation. The higher polysomal fractions were collected, treated with RNase I, and the resulting 43S-48S pre-initiation complexes and 80S species were separated in a second round of centrifugation (re-sedimentation). Isolated 80S couples were loaded in five serial two-fold dilutions onto SDS-PAGE and the amounts of the small ribosomal protein Rps0A and 80S-associated factors were analyzed by quantitative Western blotting (Figures 9 and 10; three representative, consecutive dilutions for each factor are shown; presented experiments were repeated at least 5-times).

The readthrough-increasing *rps3*-R116D mutation displayed statistically significant enrichment of eIF3, as well as both release factors eRF1 (*SUP45*) and eRF3 (*SUP35*) in heavy polysomes compared to the wt control (Figure 9A and B). Importantly, initiation and elongation factors eIF1

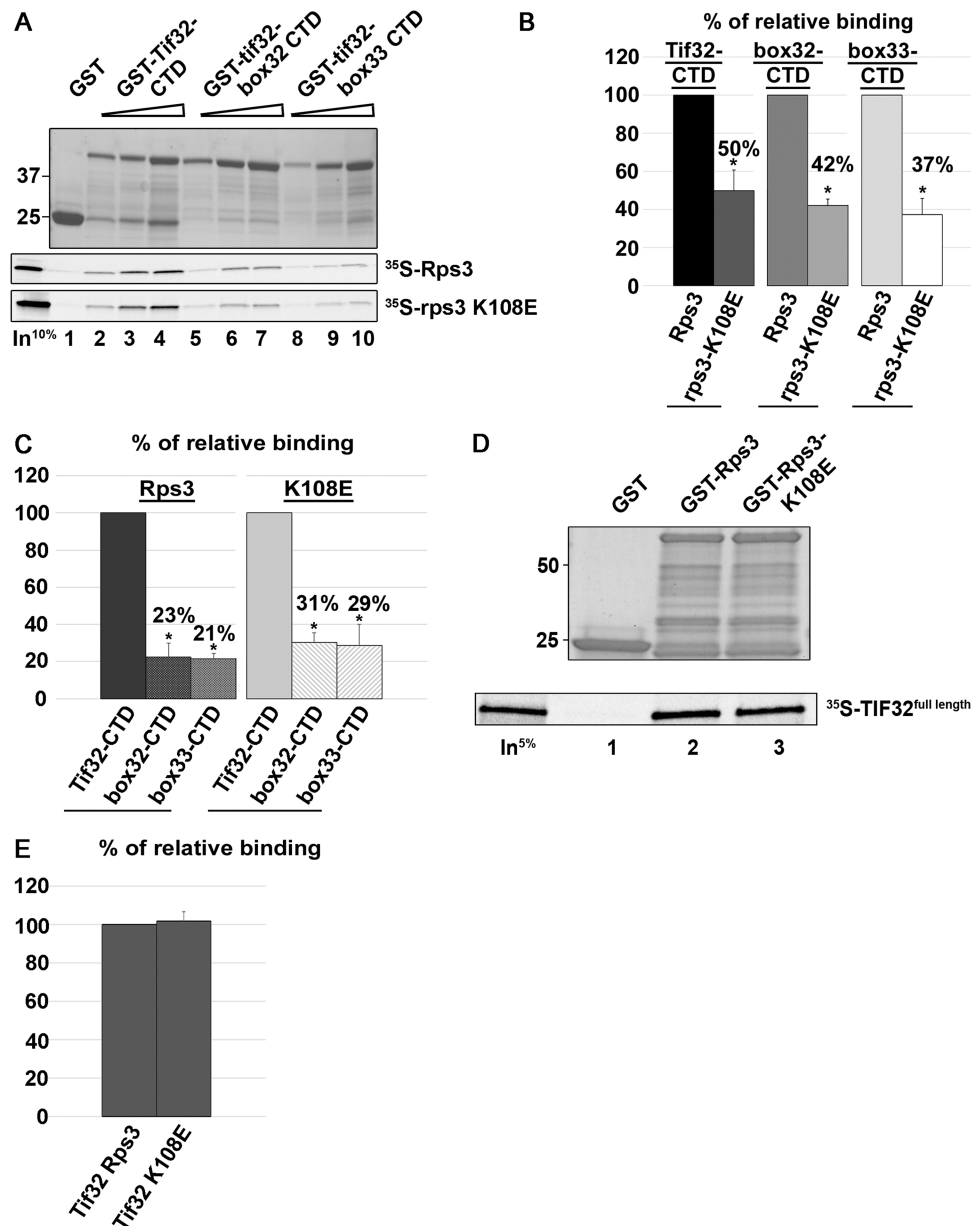


**Figure 7.** Analysis of the physical interaction between the  $\alpha$ /Tif32 C-terminal mutations and rps3-K108E. (A–E) Both *tif32-box* mutations, as well as *rps3-K108E* impair the  $\alpha$ /Tif32-Rps3 interaction independently of each other; the latter one only in the context of the  $\alpha$ /Tif32-CTD (compare A–C versus D–E). The indicated wt or mutant proteins (or their segments) were fused to the GST moiety and together with the GST alone control tested for binding to the indicated [<sup>35</sup>S]-labeled proteins or their mutant derivatives. Panel A is re-using the same control as that shown in Figure 5A. (In) indicates input amounts of proteins added to each reaction. The plots represent average values obtained from analysis of at least three independent GST-pull down experiments; standard deviations are given. Statistical significance determined by the student's *t*-test is indicated ( $P < 0.05$ ).

and eEF1A, respectively, which were used as a specificity control because neither of them imparts any termination phenotype when down-regulated (26,27), showed no significant alterations. (Residual amounts of eIF1 occurring in the 80S samples most probably reflect the existence of an eIF1-containing 'eIF3-translasome' complex proposed to associate with elongating 80S ribosomes (66)). These results suggest that heavy polysomes are enriched with terminating ribosomes in R116D, in other words that the rate of the termination reaction is slower, which may indeed result in increased stop codon readthrough.

Conversely, the *tif32-box33* mutation decreased the representation of terminating ribosomes in heavy polysomes (Figure 9A and B), which may indicate that the rate of the termination reaction is faster, perhaps due to the underrepresentation of eIF3 in pre-TCs (note that eIF3 interferes with the eRF1 role in termination (27)), which would reduce readthrough as observed (Figure 3). Combining *rps3-R116D* with *tif32-box33* seems to partially correct these opposite defects (Figure 9A and B), in agreement with the correction of the readthrough phenotype (Figure 4A). Since it does not correct the growth defect of *tif32-box33* (Figure

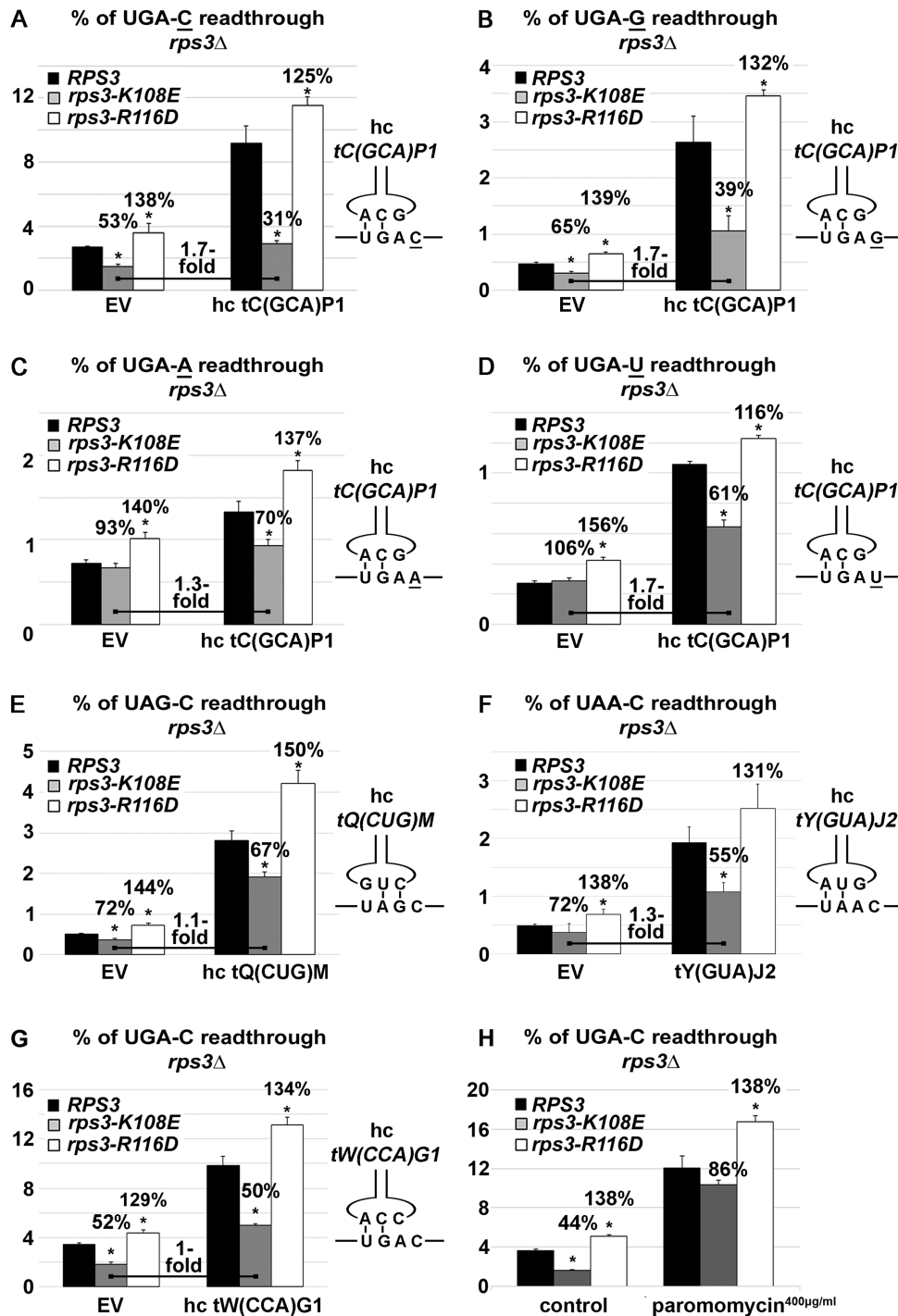


**Figure 8.** The intact K108 residue of Rps3 is important for Cys-rti-tRNA incorporation at the UGA stop codon in the +4 base-specific manner. (A–G) The *rps3*Δ strains ME166 bearing the indicated *rps3* mutant alleles on a single copy plasmid were introduced with the indicated dual luciferase readthrough reporter constructs (KP22 for UGA-C, KP35 for UGA-G, KP34 for UGA-A, KP36 for UGA-U, ZP40 for UAG-C and KP41 for UAA-C) in combination with either empty vector (EV) or indicated rti-tRNA on high copy plasmid, grown in SD and processed for stop codon readthrough measurements as described in Figure 2B. Schematics of individual rti-tRNAs base-pairing with the indicated stop codon tetranucleotides are given to the right of the plots; only the nucleotides of the anticodon loop are shown. (H) The readthrough stimulatory effect of the K108 residue requires proper conformation of the decoding center. The *rps3*Δ strains KPH126, 127 and 128 bearing the indicated *rps3* mutant alleles on a single copy plasmid were grown in SD media without or with 400 μg/ml paromomycin for six hours and processed for stop codon readthrough measurements as described in Figure 2B. Statistical significance determined by the Student’s *t*-test is indicated ( $P < 0.05$ ).

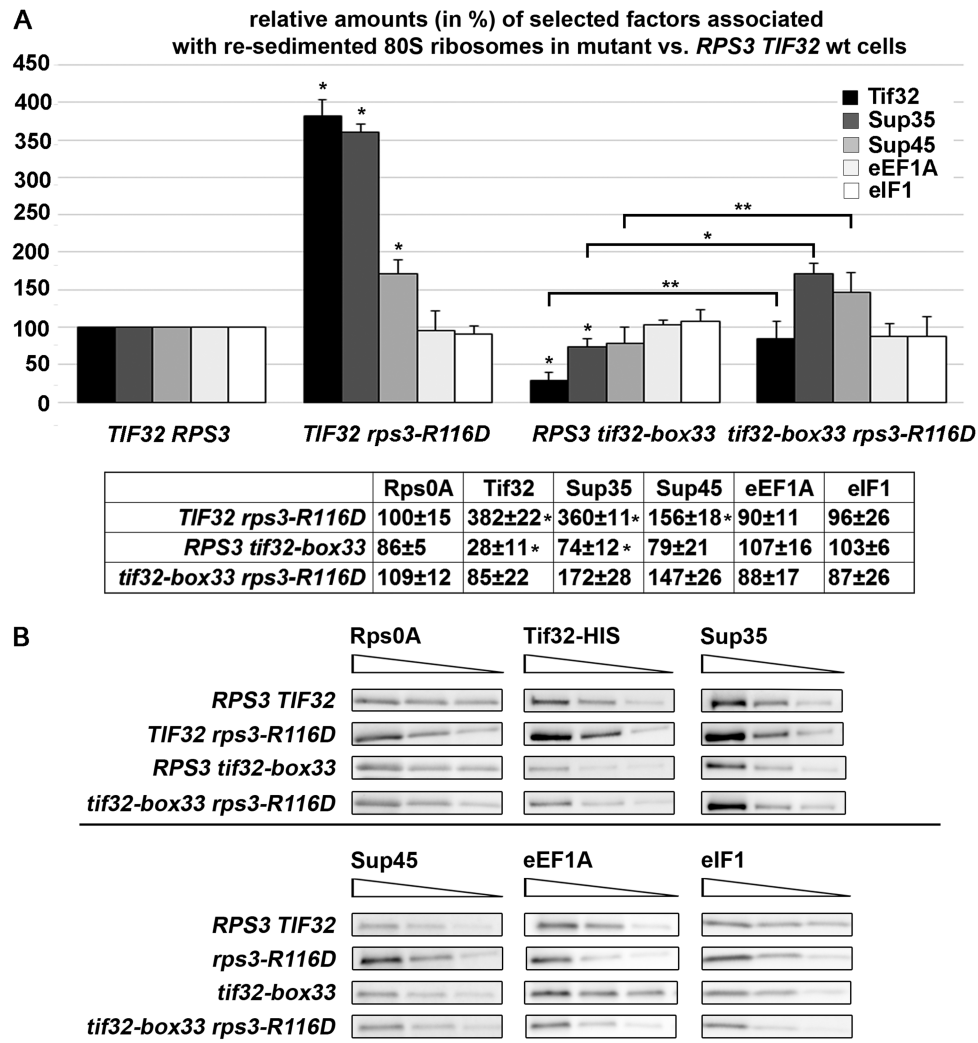


**Figure 9.** Readthrough-increasing *rps3-R116D* displays statistically significant enrichment of eIF3, eRF1 and eRF3 in heavy polysomes, whereas *tif32-Box33* reduces their amounts. (A and B) Transformants of KPH31 (*rps3Δ tif32Δ*) bearing the indicated wt or mutant *TIF32* and *RPS3* alleles were grown in the YPD medium at 30°C to an  $OD_{600} \sim 1$  and subjected to the heavy polysomal gradient resedimentation analysis followed by western blotting as described in Materials and Methods. Quantification of selected factors from at least five independent experiments shown in panel A was performed as follows. Western blot signals from each of the five 2-fold dilutions obtained with individual antibodies were quantified by Quantity One and plotted against their corresponding loadings (three representative dilutions for each factor are shown in panel B). Individual slopes (representing relative amount of each factor in mutant cells) calculated from the linear regression of resulting plots were normalized to the slope obtained with the *TIF32 RPS3* wt strain, which was set to 100%. Statistical significance determined by the student's *t*-test is indicated (\* $P < 0.05$ ; \*\* $P < 0.1$ ).

4B), we conclude that the impaired termination is not the major defect of this mutant.

The readthrough-reducing *rps3-K108E* mutation showed a statistically significant increase in the level of eRF3 (*SUP35*) in heavy polysomes without a concomitant increase in the eRF1 levels for which we do not have a rational explanation at present (Figure 10A and B). At the same time this mutant modestly reduced levels of eIF3, suggesting that eIF3 could be underrepresented in pre-TCs, which could result in decreased readthrough as explained above. Combining *rps3-K108E* with *tif32-box33* partially corrected the increase of the eRF3 levels seen with the K108E single mutant and further reduced the eIF3 levels (Figure 10A and B). The latter effect may explain why this combination exacerbated the negative readthrough phenotype of single mutants seen in Figure 6A. Virtually no difference was observed with the

control eEF1A and eIF1 factors, as well as when the control *rps3-N111A* mutant was subjected to this type of analysis (Supplementary Figure S4).

## DISCUSSION

In this study we identified two specific residues (K108 and R116) in the neighboring helices of Rps3, whose mutations to the opposite charge: (i) reduced Rps3 binding to the CTD of the  $\alpha$ /Tif32 subunit of eIF3 *in vitro*, (ii) impaired the composition of pre-termination complexes *in vivo*, (iii) affected fidelity of translation termination in the opposite manner—one decreased and the other increased efficiency of stop codon readthrough and (iv) displayed a stop codon tetranucleotide-specific impact on the ability of some rtiRNAs to efficiently incorporate into the A-site in order to

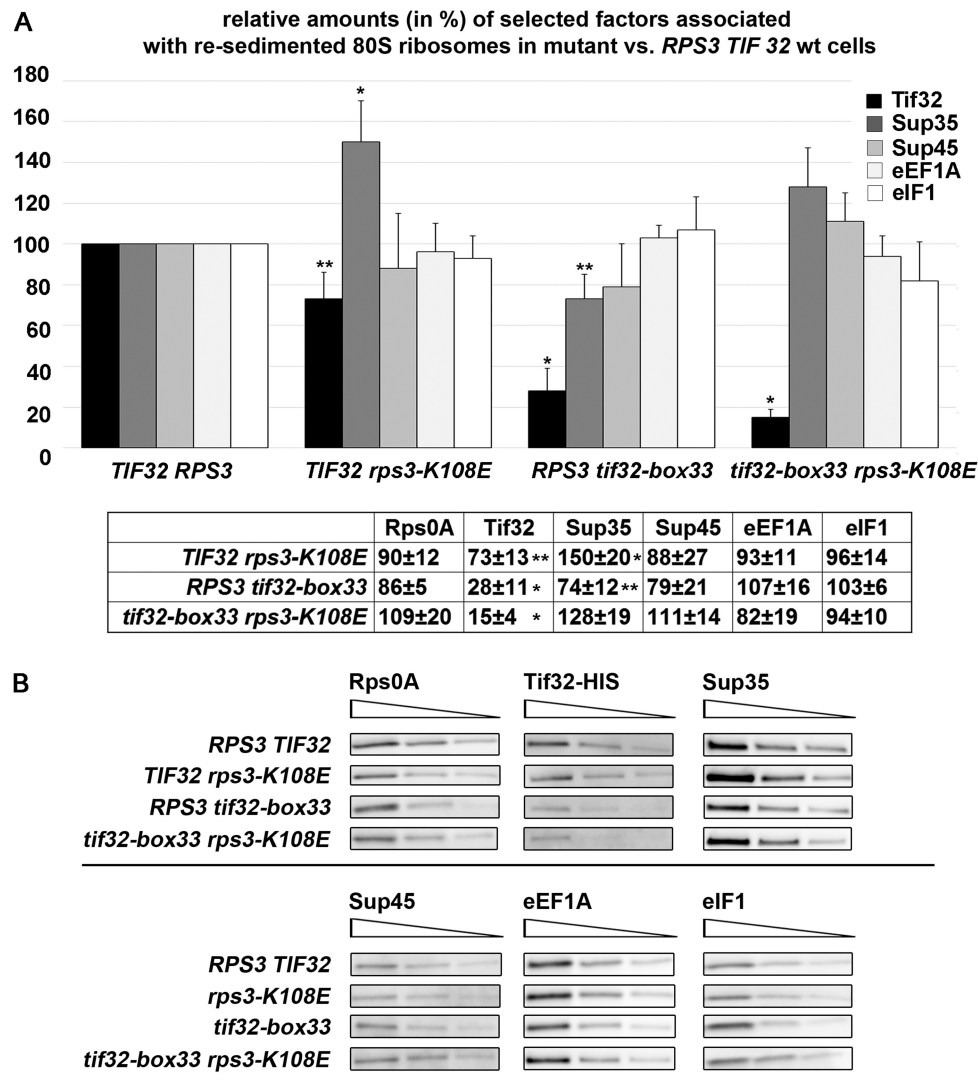


**Figure 10.** Readthrough-decreasing *rps3-K108E* displays a statistically significant increase in the level of eRF3 (*SUP35*) in heavy polysomes and, at the same time modestly reduces levels of eIF3. The same as in Figure 9 except that *rps3-K108E* was analyzed.

promote increased readthrough. In addition, we revealed that these Rps3 residues fine tune termination fidelity in close co-operation with the residues representing the very C-terminus of a/Tif32 that, when substituted with a stretch of alanine residues, reduced a/Tif32 binding to Rps3 *in vitro* and eIF3 occupancy in pre-TCs *in vivo*, and diminished the efficiency of stop codon readthrough.

In the past, mutations of basic residues in 30S ribosomal proteins uS3 and uS4 at the opening of the mRNA entry channel were implicated in the intrinsic helicase activity of the elongating 70S ribosome *in vitro* (42). In particular, it was proposed that uS3, uS4 and uS5 form a ring around the incoming mRNA and act as a processivity clamp for the ribosomal helicase function with a profound impact on the elongation rates. Among the residues identified in bacterial uS3 are those showing evolutionary conservation with K108 and R116 in yeast uS3/Rps3 (5). Hence, even though the intrinsic helicase activity of the eukaryotic ribosome has—to our knowledge—never been examined, it is theoret-

ically possible that defects in the helicase activity of the eukaryotic ribosome could stand behind (or at least contribute to) the readthrough phenotypes that we observed. However, whereas the elongation rate is by definition strongly influenced by the speed of the 80S ribosome moving in the 5' to 3' direction and encounter of secondary structures will naturally slow it down, the termination rate relies primarily on the rate of the assembly and action of release factors on the stalled ribosome and, as such, should not be influenced by its helicase activity.

Our *in vitro* protein-protein binding analysis revealed that at least 4 points of contact do exist among Rps3 and Tif32 (Figures 5 and 7). Both *rps3* mutations reduced (to varying degree) binding of rps3 to the wt a/Tif32 protein, and so did both *tif32-box* mutations in case of wt Rps3. Combining them resulted in an additive effect strongly suggesting that they are not in a mutual contact. As aforementioned, the a/Tif32-CTD forms the flexible arm under the 40S beak (Figure 3A) that is during particular initiation re-

actions able to transpose the b/Prt1-g/Tif35-i/Tif34 module from the solvent-exposed side to the decoding site and back (6,24,67,68). Hence even though the resolved density attributed to the a/Tif32-CTD residues 813 through 939 does not lie close enough to Rps3 to be able come into a direct contact (Figure 3A), it is conceivable that in the context of the terminating 80S ribosome with the decoding site occupied by the eRF1/3 complex, this a/Tif32 segment moves upwards and establishes three independent contacts with Rps3 that co-operate to modulate fidelity of termination. In addition, a/Tif32 residues 200 through 396 showed strong interaction with Rps3 that is also not mediated by the K108 and R116 residues (Figure 5). Interestingly, the same a/Tif32 segment was also shown to interact with the Rps3-neighboring uS2/Rps0 *in vitro* (69) and the entire a/Tif32-NTD displayed a strong yeast two-hybrid interaction with the beak protein eS10/Rps10 (49), which is known to make multiple contacts with the N-terminal domain of Rps3 (43). All these observations thus support the existence of the 3<sup>rd</sup> contact between a/Tif32 and Rps3, whose functional significance remains to be explored. Based on the earlier observation that direct contacts of Rps3 residues R116/R117 with mRNA nucleotides at the entry channel cooperate with eIF3 interactions at both the exit (mediated mainly by the NTD of a/Tif32 (7)) and entry channels (mediated mainly by the CTD of a/Tif32 (7)) to stabilize mRNA binding to 43S PICs (50), we can only speculate that i) a similar stabilization effect would be required also during termination to enable the termination complex to form properly, and ii) that the mutual contact between Rps3 and the a/Tif32-NTD could be an important part of it.

It is intriguing that two residues that are next to each other in parallel helices with their side chains facing into different planes displayed opposite effects on the composition of the pre-TC *in vivo*, as well as on the fidelity of termination. The K108 that highly likely contacts 18S rRNA h34 – when substituted with aspartic acid – reduced readthrough (Figure 2), showed a statistically significant increase in the level of eRF3 (*SUP35*) in heavy polysomes and, at the same time modestly reduced levels of eIF3 (Figure 10). Since the effect of this mutation on the binding affinity between full length a/Tif32 and Rps3 *in vitro* is negligible (Figure 7), we suggest that rather than mere stabilization of binding, K108 actively ensures a smooth progression of the termination process. Conversely, the R116 contacting mRNA bases 3' of the stop codon – when substituted with arginine – increased readthrough (Figure 2) and displayed statistically significant enrichment of eIF3 and both release factors in heavy polysomes (Figure 9), which may suggest that the termination rate is slower, resulting in increased readthrough efficiency. In contrast to K108E, the *rps3-R116D* mutation also reduced binding affinity towards full length a/Tif32 (Figure 5), further underscoring a clear difference in molecular functioning of these two neighboring residues. Finally, the *tif32-box33* mutation decreased the representation of terminating ribosomes in heavy polysomes; the effect was particularly strong for the eIF3 complex itself (Figure 9), which may speak for a faster rate of the termination reaction. This mutation also dramatically impaired binding of a/Tif32 to Rps3 *in vitro* (Figure 5).

What does this all mean? It is clear that both contacts represented by the K108/R116 residues on one hand and box32/33 residues on the other affect the termination reaction by different means. We think that the simplest explanation is that the latter contact is responsible for tight anchoring of eIF3 to pre-TCs. When disrupted, the eIF3 affinity towards the small subunit is reduced and the resulting underrepresentation of eIF3 in pre-TCs mitigates their intrinsic readthrough efficiency, since eIF3 can no longer interfere with the eRF1 role in termination—perhaps by impairing its proper orientation in the A-site—as observed and proposed before for other eIF3 mutants with a similar problem (26,27). The former contact is most likely more directly involved in the termination process *per se* as its disruption seems to impede progression of particular termination steps.

As mentioned above, during stop codon decoding, eRF1 was proposed to sit in the ribosomal A-site with a part of its N-domain contacting small ribosomal protein Rps3 and h18 of 18S rRNA (48). It was also proposed that in analogy to the scanning arrest relying on the closure of the 40S latch (formed by Rps3 and 18S rRNA helices 18 and 34) that clamps on the mRNA upon AUG recognition (reviewed in (2)), a similar mechanism involving similar players (Rps3 and h16 forming the beak next to h18) may operate also during the elongation arrest upon stop codon recognition (6,48). A further support for the termination-specific latch closure was provided by the work studying binding of the no-go mRNA decay complex DOM34–HBS1 to stalled yeast ribosomes where the connection between Rps3 and h16 was also observed (70). Furthermore, the +6 nt of the TISU element present in some mRNAs with very short UTRs was crosslinked to Rps3 in the 48S complex; however, upon 80S complex formation, the Rps3 interaction (constricting?) was weakened and switched to eS10/Rps10 (non-constricting?) (51). Evidence of such conformational changes at the entry channel during the transition from the 48 PIC to the elongation-competent 80S ribosome logically provoke thinking that the reversal conformational changes involving Rps3 do occur during the transition from the elongation-competent 80S ribosome to the pre-TC.

Having postulated that, we speculate that K108 functions to sense the presence of eRF1 in the pre-TC to timely close the ‘termination’ latch. We further propose that by contacting K108, eIF3 modulates this role in such a way to delay the latch closure to promote programmed stop codon readthrough. If K108 is substituted with aspartic acid, the functional impairment of the Rps3–a/Tif32 contact, and perhaps also of that between Rps3 and h34, weakens and/or alters the influence of eIF3 and Rps3 over eRF1 and thus allows the termination-specific constriction of the latch to occur ‘prematurely’. This would in turn decrease readthrough, as was observed (Figure 6). In agreement, combining *rps3-K108E* with *tif32-box33* exacerbated the efficiency of readthrough of individual mutants and further reduced the eIF3 levels in pre-TCs. As K108E was recently shown to allow frameshifting at inhibitory CGA-CGA codon pairs (41), we believe that the K108 influence over the latch mechanism could also explain how K108 prevents frameshifting; simply by keeping it in a proper,

elongation-specific conformation (provided that alterations of the latch mechanism accompany frameshifting).

In case of R116D, we propose that the dominant defect is the loss of the Rps3 contact with mRNA's bases downstream of stop codon in the mRNA entry channel. In analogy with the helicase activity (formation of a ring around the incoming mRNA acting as a processivity clamp), we think that increased readthrough arises from the failure of rps3-R116D to provide electrostatic attraction for the phosphate backbone of mRNA with its stop codon in the A-site that would clamp it into the entry channel as a part of the constriction movement. This way the terminating ribosome would be locked in a non-productive state—the latch constriction would not properly materialize—with release factors unable to accommodate properly in the A-site. This could lead to their increased on and off rate, which would together with the observed concomitant increase in the eIF3 abundance (perhaps due to the impairment of one of its three contacts with Rps3 that might be required for its timely departure or relocation) allow rti-tRNAs to incorporate into the A-site and thus increase the rate of readthrough. In support, the R116D mutant was proposed to destabilize the closed/entry channel-constricted conformation of the initiating, scanning-arrested 48S PIC and as a result to increase discrimination against initiation on near-cognate initiation codons (50). Destabilization of the closed 48S PIC conformation was also observed with specific a/Tif32 mutations lying upstream of box32, as well as with some mutations in g/Tif35 which also interacts with Rps3 (8,12). However, taking into account the eIF3 stimulatory role in readthrough (26,27), we cannot rule out that the R116D-derived increased readthrough stems solely from a simple stabilization of eIF3 in the R116D pre-TCs. In agreement with both options, combining *rps3-R116D* with *tif32-box33* apparently relieved the readthrough stimulatory effect of wt eIF3 as it fully suppressed the R116D-derived increased readthrough (Figure 4) and even partially corrected the eRFs accumulation phenomenon (Figure 9). Noteworthy, the R116A mutation was recently shown to impair the No-go Decay that Rps3 together with Dom34 and Asc1 promotes (71).

Finally, we found that K108 but not R116 affects efficiency of termination/stop codon readthrough in the stop codon tetranucleotide manner and promotes incorporation of Cys-rti-tRNAs (and to a smaller degree also that of Tyr-rti-tRNA) (Figure 8A–G). Taking into account that R116 but not K108 interacts with mRNA in the entry pore and, as such, could have a direct influence over sensing the stop codon context (in fact, R116D was shown to increase discrimination against an AUG codon in suboptimal Kozak context (50)), it was unexpected that we observed specific effects only with the K108E mutant. Nonetheless, since the similar tetranucleotide-specific phenotype was found to be associated with several eIF3 mutants (26,27) and proposed to occur allosterically by altering the position of the A1493 phosphate group in the decoding pocket (6), we speculate that the sensing may occur in co-operation between these two proteins, perhaps via h34 of 18S rRNA. In support, paromomycin treatment (destabilizing the geometry of the decoding pocket) neutralized the stimulatory effect of K108 on stop codon readthrough practically to the same extent as

that shown before for eIF3 (Figure 8H) (26,27). In contrast, it had no influence on the R116D effect strongly suggesting that R116 operates in a different manner that is not dependent on the proper conformation of the A-site.

Considering that readthrough is linked to human disease—more than 15% of all human genetic diseases can be attributed to the presence of a premature stop codon (PTC) in the coding region of an essential protein (72) and for thus-mutated mRNAs the frequency of readthrough basically defines the efficiency of functional protein synthesis (73)—we believe that findings presented in this study further deepen our knowledge of this important regulatory mechanism of gene expression.

## SUPPLEMENTARY DATA

Supplementary Data are available at NAR Online.

## ACKNOWLEDGEMENTS

We are thankful to Laxminarayana Burela from Alan Hinnebusch's lab for his help with cloning and initial phenotypic testing of a/Tif32 mutants, to Melissa J. Moore and Elizabeth J. Grayhack for timely gifts of material, to Olga Krýdová and Veronika Kovaničová for technical and administrative assistance, and to the members of the Valášek, Krásný, Staněk and Svoboda laboratories for helpful suggestions. This work made a use of the imaging instrument provided by the C4Sys infrastructure.

## FUNDING

Czech Science Foundation [18-02014S to L.S.V.]; GA UK project [280217 to K.P., in part]. Funding for open access charge: Czech Science Foundation [18-02014S].

*Conflict of interest statement.* None declared.

## REFERENCES

- Valášek, L.S. (2012) 'Ribozoomin' – translation initiation from the perspective of the ribosome-bound eukaryotic initiation factors (eIFs). *Curr. Protein Pept. Sci.*, **13**, 305–330.
- Hinnebusch, A.G. (2017) Structural insights into the mechanism of scanning and start codon recognition in eukaryotic translation initiation. *Trends Biochem. Sci.*, **42**, 589–611.
- Jackson, R.J., Hellen, C.U. and Pestova, T.V. (2012) Termination and post-termination events in eukaryotic translation. *Adv. Protein Chem. Struct. Biol.*, **86**, 45–93.
- Wilson, D.N. and Doudna, J.H. (2012) The structure and function of the eukaryotic ribosome. *Cold Spring Harbor Perspect. Biol.*, **4**, 1–17.
- Graifer, D. and Karpova, G. (2015) Roles of ribosomal proteins in the functioning of translational machinery of eukaryotes. *Biochimie.*, **109**, 1–17.
- Valášek, L.S., Zeman, J., Wagner, S., Beznoskova, P., Pavlikova, Z., Mohammad, M.P., Hronova, V., Herrmannova, A., Hashem, Y. and Gunisova, S. (2017) Embraced by eIF3: structural and functional insights into the roles of eIF3 across the translation cycle. *Nucleic Acids Res.*, **45**, 10948–10968.
- Aitken, C.E., Beznoskova, P., Vlckova, V., Chiu, W.L., Zhou, F., Valasek, L.S., Hinnebusch, A.G. and Lorsch, J.R. (2016) Eukaryotic translation initiation factor 3 plays distinct roles at the mRNA entry and exit channels of the ribosomal preinitiation complex. *Elife*, **5**, e20934.
- Cuchalová, L., Kouba, T., Herrmannová, A., Danyi, I., Chiu, W.-l and Valášek, L. (2010) The RNA recognition motif of eukaryotic

- translation initiation factor 3g (eIF3g) is required for resumption of scanning of posttermination ribosomes for reinitiation on GCN4 and together with eIF3i stimulates linear scanning. *Mol. Cell Biol.*, **30**, 4671–4686.
9. Khoshnevis, S., Gunišová, S., Vlčková, V., Kouba, T., Neumann, P., Beznosková, P., Ficner, R. and Valášek, L.S. (2014) Structural integrity of the PCI domain of eIF3a/TIF32 is required for mRNA recruitment to the 43S pre-initiation complexes. *Nucleic Acids Res.*, **42**, 4123–4139.
  10. Kouba, T., Rutkai, E., Karasková, M. and Valášek, L.S. (2012) The eIF3c/NIP1 PCI domain interacts with RNA and RACK1/ASC1 and promotes assembly of the pre-initiation complexes. *Nucleic Acids Res.*, **40**, 2683–2699.
  11. Karaskova, M., Gunišova, S., Herrmannova, A., Wagner, S., Munzarova, V. and Valasek, L.S. (2012) Functional characterization of the role of the N-terminal domain of the c/Nip1 subunit of eukaryotic initiation factor 3 (eIF3) in AUG recognition. *J. Biol. Chem.*, **287**, 28420–28434.
  12. Chiu, W.-L., Wagner, S., Herrmannová, A., Burela, L., Zhang, F., Saini, A.K., Valášek, L. and Hinnebusch, A.G. (2010) The C-terminal region of eukaryotic translation initiation factor 3a (eIF3a) promotes mRNA recruitment, scanning, and, together with eIF3j and the eIF3b RNA recognition motif, selection of AUG start codons. *Mol. Cell Biol.*, **30**, 4415–4434.
  13. Wagner, S., Herrmannova, A., Malik, R., Peclinovska, L. and Valasek, L.S. (2014) Functional and biochemical characterization of human eukaryotic translation initiation factor 3 in living cells. *Mol. Cell Biol.*, **34**, 3041–3052.
  14. Herrmannová, A., Daujotyte, D., Yang, J.C., Cuchalová, L., Gorrec, F., Wagner, S., Danyi, I., Lukavsky, P.J. and Valášek, L.S. (2012) Structural analysis of an eIF3 subcomplex reveals conserved interactions required for a stable and proper translation pre-Initiation complex assembly. *Nucleic Acids Res.*, **40**, 2294–2311.
  15. Wagner, S., Herrmannova, A., Sikrova, D. and Valasek, L.S. (2016) Human eIF3b and eIF3a serve as the nucleation core for the assembly of eIF3 into two interconnected modules: the yeast-like core and the octamer. *Nucleic Acids Res.*, **44**, 10772–10788.
  16. Sun, C., Querol-Audi, J., Mortimer, S.A., Arias-Palomo, E., Doudna, J.A., Nogales, E. and Cate, J.H. (2013) Two RNA-binding motifs in eIF3 direct HCV IRES-dependent translation. *Nucleic Acids Res.*, **41**, 7512–7521.
  17. Smith, M.D., Gu, Y., Querol-Audi, J., Vogan, J.M., Nitido, A. and Cate, J.H. (2013) Human-like eukaryotic translation initiation factor 3 from *Neurospora crassa*. *PLoS One*, **8**, e78715.
  18. Kovarik, P., Hašek, J., Valášek, L. and Ruis, H. (1998) RPB1: an essential gene of *Saccharomyces cerevisiae* encoding a 110-kDa protein required for passage through the G1 phase. *Curr. Genet.*, **33**, 100–109.
  19. Lee, A.S., Kranzusch, P.J. and Cate, J.H. (2015) eIF3 targets cell-proliferation messenger RNAs for translational activation or repression. *Nature*, **522**, 111–114.
  20. Villa, N., Do, A., Hershey, J.W. and Fraser, C.S. (2013) Human eukaryotic initiation factor 4G (eIF4G) binds to eIF3c, -d, and -e to promote mRNA recruitment to the ribosome. *J. Biol. Chem.*, **288**, 32932–32940.
  21. Sokabe, M., Fraser, C.S. and Hershey, J.W.B. (2011) The human translation initiation multi-factor complex promotes methionyl-tRNA<sub>i</sub> binding to the 40S ribosomal subunit. *Nucleic Acids Res.*, **40**, 905–913.
  22. des Georges, A., Dhote, V., Kuhn, L., Hellen, C.U., Pestova, T.V., Frank, J. and Hashem, Y. (2015) Structure of mammalian eIF3 in the context of the 43S preinitiation complex. *Nature*, **525**, 491–495.
  23. Pisareva, V.P. and Pisarev, A.V. (2016) DHX29 and eIF3 cooperate in ribosomal scanning on structured mRNAs during translation initiation. *RNA*, **22**, 1859–1870.
  24. Llacer, J.L., Hussain, T., Saini, A.K., Nanda, J.S., Kaur, S., Gordiyenko, Y., Kumar, R., Hinnebusch, A.G., Lorsch, J.R. and Ramakrishnan, V. (2018) Translational initiation factor eIF5 replaces eIF1 on the 40S ribosomal subunit to promote start-codon recognition. *Elife*, **7**, e39273.
  25. Asano, K., Phan, L., Valasek, L., Schoenfeld, L.W., Shalev, A., Clayton, J., Nielsen, K., Donahue, T.F. and Hinnebusch, A.G. (2001) A multifactor complex of eIF1, eIF2, eIF3, eIF5, and tRNA(i)Met promotes initiation complex assembly and couples GTP hydrolysis to AUG recognition. *Cold Spring Harb. Symp. Quant. Biol.*, **66**, 403–415.
  26. Beznosková, P., Cuchalová, L., Wagner, S., Shoemaker, C.J., Gunišová, S., Von der Haar, T. and Valášek, L.S. (2013) Translation initiation factors eIF3 and HCR1 control translation termination and stop codon read-through in yeast cells. *PLoS Genet.*, **9**, e1003962.
  27. Beznoskova, P., Wagner, S., Jansen, M.E., von der Haar, T. and Valasek, L.S. (2015) Translation initiation factor eIF3 promotes programmed stop codon readthrough. *Nucleic Acids Res.*, **43**, 5099–5111.
  28. Shoemaker, C.J. and Green, R. (2011) Kinetic analysis reveals the ordered coupling of translation termination and ribosome recycling in yeast. *Proc. Natl. Acad. Sci. U.S.A.*, **108**, E1392–E1398.
  29. Schuller, A.P. and Green, R. (2018) Roadblocks and resolutions in eukaryotic translation. *Nat. Rev. Mol. Cell Biol.*, **19**, 526–541.
  30. Dabrowski, M., Bukowy-Bieryllo, Z. and Zietkiewicz, E. (2015) Translational readthrough potential of natural termination codons in eucaryotes—The impact of RNA sequence. *RNA Biol.*, **12**, 950–958.
  31. Schueren, F. and Thoms, S. (2016) Functional translational readthrough: a systems biology perspective. *PLoS Genet.*, **12**, e1006196.
  32. Tate, W.P., Cridge, A.G. and Brown, C.M. (2018) ‘Stop’ in protein synthesis is modulated with exquisite subtlety by an extended RNA translation signal. *Biochem. Soc. Trans.*, **46**, 1615–1625.
  33. Beznoskova, P., Gunisova, S. and Valasek, L.S. (2016) Rules of UGA-N decoding by near-cognate tRNAs and analysis of readthrough on short uORFs in yeast. *RNA*, **22**, 456–466.
  34. Gunisova, S., Beznoskova, P., Mohammad, M.P., Vlckova, V. and Valasek, L.S. (2016) In-depth analysis of cis-determinants that either promote or inhibit reinitiation on GCN4 mRNA after translation of its four short uORFs. *RNA*, **22**, 542–558.
  35. Beznoskova, P., Pavlikova, Z., Zeman, J., Echeverria Aitken, C. and Valasek, L.S. (2019) Yeast applied readthrough inducing system (YARIS): an invivo assay for the comprehensive study of translational readthrough. *Nucleic Acids Res.*, **47**, 6339–6350.
  36. Brown, A., Shao, S., Murray, J., Hegde, R.S. and Ramakrishnan, V. (2015) Structural basis for stop codon recognition in eukaryotes. *Nature*, **524**, 493–496.
  37. Matheisl, S., Berninghausen, O., Becker, T. and Beckmann, R. (2015) Structure of a human translation termination complex. *Nucleic Acids Res.*, **43**, 8615–8626.
  38. Bowen, A.M., Musalgaonkar, S., Moomau, C.A., Gulay, S.P., Mirvis, M. and Dinman, J.D. (2015) Ribosomal protein uS19 mutants reveal its role in coordinating ribosome structure and function. *Translation (Austin)*, **3**, e1117703.
  39. Landry, D.M., Hertz, M.I. and Thompson, S.R. (2009) RPS25 is essential for translation initiation by the Dicistroviridae and hepatitis C viral IRESs. *Genes Dev.*, **23**, 2753–2764.
  40. Hendrick, J.L., Wilson, P.G., Edelman, II, Sandbaken, M.G., Ursic, D. and Culbertson, M.R. (2001) Yeast frameshift suppressor mutations in the genes coding for transcription factor Mbf1p and ribosomal protein S3: evidence for autoregulation of S3 synthesis. *Genetics*, **157**, 1141–1158.
  41. Wang, J., Zhou, J., Yang, Q. and Grayhack, E.J. (2018) Multi-protein bridging factor 1 (Mbf1), Rps3 and Asc1 prevent stalled ribosomes from frameshifting. *Elife*, **7**, e39637.
  42. Takyar, S., Hickerson, R.P. and Noller, H.F. (2005) mRNA helicase activity of the ribosome. *Cell*, **120**, 49–58.
  43. Graifer, D., Malygin, A., Zharkov, D.O. and Karpova, G. (2014) Eukaryotic ribosomal protein S3: a constituent of translational machinery and an extraribosomal player in various cellular processes. *Biochimie*, **99**, 8–18.
  44. Pisarev, A.V., Kolupaeva, V.G., Yusupov, M.M., Hellen, C.U.T. and Pestova, T.V. (2008) Ribosomal position and contacts of mRNA in eukaryotic translation initiation complexes. *EMBO J.*, **27**, 1609–1621.
  45. Molotkov, M.V., Graifer, D.M., Popugaeva, E.A., Bulygin, K.N., Meschaninova, M.I., Ven'yaminova, A.G. and Karpova, G.G. (2006) mRNA 3' of the A site bound codon is located close to protein S3 on the human 80S ribosome. *RNA Biol.*, **3**, 122–129.
  46. Hussain, T., Llacer, J.L., Fernandez, I.S., Munoz, A., Martin-Marcos, P., Savva, C.G., Lorsch, J.R., Hinnebusch, A.G. and Ramakrishnan, V. (2014) Structural changes enable start codon recognition by the eukaryotic translation initiation complex. *Cell*, **159**, 597–607.

47. Passmore, L.A., Schmeing, T.M., Maag, D., Applefield, D.J., Acker, M.G., Algire, M.A., Lorsch, J.R. and Ramakrishnan, V. (2007) The eukaryotic translation initiation factors eIF1 and eIF1A induce an open conformation of the 40S ribosome. *Mol. Cell*, **26**, 41–50.
48. Taylor, D., Unbehauen, A., Li, W., Das, S., Lei, J., Liao, H.Y., Grassucci, R.A., Pestova, T.V. and Frank, J. (2012) Cryo-EM structure of the mammalian eukaryotic release factor eRF1-eRF3-associated termination complex. *Proc. Natl. Acad. Sci. U.S.A.*, **109**, 18413–18418.
49. Valášek, L., Mathew, A., Shin, B.S., Nielsen, K.H., Szamecz, B. and Hinnebusch, A.G. (2003) The yeast eIF3 subunits TIF32/a and NIP1/c and eIF5 make critical connections with the 40S ribosome in vivo. *Genes Dev.*, **17**, 786–799.
50. Dong, J., Aitken, C.E., Thakur, A., Shin, B.S., Lorsch, J.R. and Hinnebusch, A.G. (2017) Rps3/uS3 promotes mRNA binding at the 40S ribosome entry channel and stabilizes preinitiation complexes at start codons. *Proc. Natl. Acad. Sci. U.S.A.*, **114**, E2126–E2135.
51. Haimov, O., Sinvani, H., Martin, F., Ulitsky, I., Emmanuel, R., Tamarkin-Ben-Harush, A., Vardy, A. and Dikstein, R. (2017) Efficient and accurate translation initiation directed by TISU Involves RPS3 and RPS10e binding and differential eukaryotic initiation factor 1A regulation. *Mol. Cell Biol.*, **37**, e00150-17.
52. Grentzmann, G., Ingram, J.A., Kelly, P.J., Gesteland, R.F. and Atkins, J.F. (1998) A dual-luciferase reporter system for studying recoding signals. *RNA*, **4**, 479–486.
53. Muhrad, D. and Parker, R. (1999) Recognition of yeast mRNAs as 'nonsense containing' leads to both inhibition of mRNA translation and mRNA degradation: implications for the control of mRNA decapping. *Mol. Biol. Cell*, **10**, 3971–3978.
54. Keeling, K.M., Lanier, J., Du, M., Salas-Marco, J., Gao, L., Kaenjak-Angeletti, A. and Bedwell, D.M. (2004) Leaky termination at premature stop codons antagonizes nonsense-mediated mRNA decay in *S. cerevisiae*. *RNA*, **10**, 691–703.
55. Loughran, G., Howard, M.T., Firth, A.E. and Atkins, J.F. (2017) Avoidance of reporter assay distortions from fused dual reporters. *RNA*, **23**, 1285–1289.
56. Merritt, G.H., Naemi, W.R., Mugnier, P., Webb, H.M., Tuite, M.F. and von der Haar, T. (2010) Decoding accuracy in eRF1 mutants and its correlation with pleiotropic quantitative traits in yeast. *Nucleic Acids Res.*, **38**, 5479–5492.
57. Ferreira-Cerca, S., Poll, G., Kuhn, H., Neueder, A., Jakob, S., Tschochner, H. and Milkereit, P. (2007) Analysis of the in vivo assembly pathway of eukaryotic 40S ribosomal proteins. *Mol. Cell*, **28**, 446–457.
58. Limoncelli, K.A., Merrih, C.N. and Moore, M.J. (2017) ASC1 and RPS3: new actors in 18S nonfunctional rRNA decay. *RNA*, **23**, 1946–1960.
59. Bonetti, B., Fu, L., Moon, J. and Bedwell, D.M. (1995) The efficiency of translation termination is determined by a synergistic interplay between upstream and downstream sequences in *Saccharomyces cerevisiae*. *J. Mol. Biol.*, **251**, 334–345.
60. Skuzeski, J.M., Nichols, L.M., Gesteland, R.F. and Atkins, J.F. (1991) The signal for a leaky UAG stop codon in several plant viruses includes the two downstream codons. *J. Mol. Biol.*, **218**, 365–373.
61. Namy, O., Duchateau-Nguyen, G. and Rousset, J.P. (2002) Translational readthrough of the PDE2 stop codon modulates cAMP levels in *Saccharomyces cerevisiae*. *Mol. Microbiol.*, **43**, 641–652.
62. Zeman, J., Itoh, Y., Kukacka, Z., Rosulek, M., Kavan, D., Kouba, T., Jansen, M.E., Mohammad, M.P., Novak, P. and Valasek, L.S. (2019) Binding of eIF3 in complex with eIF5 and eIF1 to the 40S ribosomal subunit is accompanied by dramatic structural changes. *Nucleic Acids Res.*, **47**, 8282–8300.
63. Valášek, L., Nielsen, K.H. and Hinnebusch, A.G. (2002) Direct eIF2-eIF3 contact in the multifactor complex is important for translation initiation in vivo. *EMBO J.*, **21**, 5886–5898.
64. Bidou, L., Allamand, V., Rousset, J.P. and Namy, O. (2012) Sense from nonsense: therapies for premature stop codon diseases. *Trends Mol. Med.*, **18**, 679–688.
65. Valášek, L., Szamecz, B., Hinnebusch, A.G. and Nielsen, K.H. (2007) In vivo stabilization of preinitiation complexes by formaldehyde cross-linking. *Methods Enzymol.*, **429**, 163–183.
66. Sha, Z., Brill, L.M., Cabrera, R., Kleinfeld, O., Scheliga, J.S., Glickman, M.H., Chang, E.C. and Wolf, D.A. (2009) The eIF3 interactome reveals the translatome, a supercomplex linking protein synthesis and degradation machineries. *Mol. Cell*, **36**, 141–152.
67. Simonetti, A., Brito Querido, J., Myasnikov, A.G., Mancera-Martinez, E., Renaud, E., Kuhn, L. and Hasem, Y. (2016) eIF3 peripheral subunits rearrangement after mRNA binding and start-codon recognition. *Mol. Cell*, **63**, 206–217.
68. Mancera-Martinez, E., Brito Querido, J., Valasek, L.S., Simonetti, A. and Hasem, Y. (2017) ABCE1: A special factor that orchestrates translation at the crossroad between recycling and initiation. *RNA Biol.*, **14**, 1279–1285.
69. Kouba, T., Danyi, I., Gunišová, S., Munzarová, V., Vlčková, V., Cuchalová, L., Neueder, A., Milkereit, P. and Valášek, L.S. (2012) Small ribosomal protein RPS0 stimulates translation initiation by mediating 40S-binding of eIF3 via its direct contact with the eIF3a/TIF32 subunit. *PLoS One*, **7**, e40464.
70. Becker, T., Armache, J.P., Jarasch, A., Anger, A.M., Villa, E., Sieber, H., Motaal, B.A., Mielke, T., Berninghausen, O. and Beckmann, R. (2011) Structure of the no-go mRNA decay complex Dom34-Hbs1 bound to a stalled 80S ribosome. *Nat. Struct. Mol. Biol.*, **18**, 715–720.
71. Simms, C.L., Kim, K.Q., Yan, L.L., Qiu, J. and Zaher, H.S. (2018) Interactions between the mRNA and Rps3/uS3 at the entry tunnel of the ribosomal small subunit are important for no-go decay. *PLoS Genet.*, **14**, e1007818.
72. Linde, L. and Kerem, B. (2008) Introducing sense into nonsense in treatments of human genetic diseases. *Trends Genet.*, **24**, 552–563.
73. Keeling, K.M., Xue, X., Gunn, G. and Bedwell, D.M. (2014) Therapeutics based on stop codon readthrough. *Annu. Rev. Genomics Hum. Genet.*, **15**, 371–394.